4.4. Biological function of DDB2 ubiquitylation

As mentioned above, DDB2 protein is rapidly degraded after UV-irradiation in vivo [21,22] and we showed here that the DDB–Cul4A complex could directly ubiquitylate DDB2. What is the function of DDB2 ubiquitylation and subsequent degradation? After damaged-DNA recognition, DDB is thought to hand over the DNA lesion to the following NER component(s) including XPC [2]. An appealing hypothesis is that clearance of DDB2 by ubiquitylation and succeeding degradation facilitates accession of the following NER factor(s) to the DNA lesion. However, it is not clear at present whether the ubiquitylation of DDB2 is only required for its UV-induced degradation, or is essential to change some biological character of DDB2 preceding degradation. Because various non-proteolytic functions of ubiquitylation have been identified recently [44], it is still conceivable that the ubiquitylation of DDB2 might have an additional role besides degradation. Moreover, we still do not know whether DDB2 ubiquitylation is a pertinent event for DDB function in DNA repair, or is the only side effect accompanied by ubiquitylation of authentic, relevant substrate. To define the precise role of DDB–Cullin 4A complex-mediated ubiquitylation, further studies are obviously required; especially the identification of the physiological substrate. Such experiments are currently underway in our laboratories.

Acknowledgements

We are grateful to Dr. Yoshihiro Nakatani of Harvard Medical School for providing HeLa cells expressing epitope-tagged DDB2 and to Dr. Kaoru Sugasawa of RIKEN for the critical reading of the manuscript. We also thank all members of Prof. K. Tanaka laboratory for the helpful discussions. This work was supported by CREST of Japan Science and Technology (JST), Takeda Science Foundation (to M.S.) and Grants-in-Aid from the Ministry of Education, Culture, Sports, Science and Technology of Japan (to K.T.).

References

[1] R.S. Feldberg, L. Grossman, A DNA binding protein from human placenta specific for ultraviolet damaged DNA, Biochemistry 15 (1976) 2402–2408.
[2] J. Tang, G. Chu, Xeroderma pigmentosum complementation group E and UV-damaged DNA-binding protein, DNA Repair 1 (2002) 601–616.
[3] B.B.O. Wittschieben, R.D. Wood, DDB complexities, DNA Repair 2 (2003) 1065–1069.
[4] D. Bootsma, K.H. Kraemer, J.E. Cleaver, J.H.J. Hoeijmakers, Nucleotide excision repair syndromes: xeroderma pigmentosum, Cockayne syndrome and trichothiodystrophy, in: B. Vogelstein, K.W. Kinzler (Eds.), The Genetic Basis of Human Cancer, McGraw Hill, New York, 1997, pp. 245–274.
[5] G. Chu, E. Chang, Xeroderma pigmentosum group E cells lack a nuclear factor that binds to damaged DNA, Science 242 (1988) 564–567.
[6] B.J. Hwang, S. Toering, U. Francke, G. Chu, p48 activates a UV-damaged-DNA binding factor and is defective in xeroderma pigmentosum group E cells that lack binding activity, Mol. Cell. Biol. 18 (1998) 4391–4399.
[7] S. Keeney, A.P. Eker, T. Brody, W. Vermeulen, D. Bootsma, J.H. Hoeijmakers, S. Linn, Correction of the DNA repair defect in xeroderma pigmentosum group E by injection of a DNA damage-binding protein, Proc. Natl. Acad. Sci. U.S.A. 91 (1994) 4053–4056.
[8] V. Rapic-Otrin, I. Kuraoka, T. Nardo, M. McLenigan, A.P. Eker, M. Stefanini, A.S. Levine, R.D. Wood, Relationship of the xeroderma pigmentosum group E DNA repair defect to the chromatin and DNA binding proteins UV-DDB and replication protein A, Mol. Cell. Biol. 18 (1998) 3182–3190.
[9] J.Y. Tang, B.J. Hwang, J.M. Ford, P.C. Hanawalt, G. Chu, Xeroderma pigmentosum p48 gene enhances global genomic repair and suppresses UV-induced mutagenesis, Mol. Cells 5 (2000) 737–744.
[10] A.F. Nichols, P. Ong, S. Linn, Mutations specific to the xeroderma pigmentosum group E Ddb-phenotype, J. Biol. Chem. 271 (1996) 24317–24320.
[11] T. Itoh, S. Linn, T. Ono, M. Yamaizumi, Reinvestigation of the classification of five cell strains of xeroderma pigmentosum group E with reclassification of three of them, J. Invest. Dermatol. 114 (2000) 1022–1029.
[12] V. Rapic-Otrin, V. Navazza, T. Nardo, E. Botta, M. McLenigan, D.C. Bisi, A.S. Levine, M. Stefanini, True XP group E patients have a defective UV-damaged DNA binding protein complex and mutations in DDB2 which reveal the functional domains of its p48 product, Hum. Mol. Genet. 12 (2003) 1507–1522.
[13] P. Shiyanov, A. Nag, P. Raychaudhuri, Cullin 4A associates with the UV-damaged DNA-binding protein DDB, J. Biol. Chem. 274 (1999) 35309–35312.
[14] N. Zheng, B.A. Schulman, L. Song, J.J. Miller, P.D. Jeffrey, P. Wang, C. Chu, D.M. Koepp, S.J. Elledge, M. Pagano, R.C. Conaway, J.W. Conaway, J.W. Harper, N.P. Pavletich, Structure of the Cul1-Rbx1-Skp1-F boxSkp2 SCF ubiquitin ligase complex, Nature 416 (2002) 703–709.
[15] X. Chen, Y. Zhang, L. Douglas, P. Zhou, UV-damaged DNA-binding proteins are targets of CUL-4A-mediated ubiquitination and degradation, J. Biol. Chem. 276 (2001) 48175–48182.
[16] A. Nag, T. Bondar, S. Shiv, P. Raychaudhuri, The xeroderma pigmentosum group E gene product DDB2 is a specific target of cullin 4A in mammalian cells, Mol. Cell. Biol. 21 (2001) 6738–6747.
[17] R. Groisman, J. Polanowska, I. Kuraoka, J. Sawada, M. Saijo, R. Drapkin, A.F. Kisselev, K. Tanaka, Y. Nakatani, The ubiquitin ligase activity in the DDB2 and CSA complexes is differentially regulated by the COP9 signalosome in response to DNA damage, Cell 113 (2003) 357–367.
[18] C. Liu, K.A. Powell, K. Mundt, L. Wu, A.M. Carr, T. Caspari, Cop9/signalosome subunits and Pcu4 regulate ribonucleotide reductase by both checkpoint-dependent and -independent mechanisms, Genes Dev. 17 (2003) 1130–1140.
[19] T. Bondar, A. Ponomarev, P. Raychaudhuri, Ddb1 is required for the proteolysis of the *Schizosaccharomyces pombe* replication inhibitor Spd1 during S phase and after DNA damage, J. Biol. Chem. 279 (2004) 9937–9943.
[20] I.E. Wertz, K.M. O'Rourke, Z. Zhang, D. Dornan, D. Arnott, R.J. Deshaies, V.M. Dixit, Human De-etiolated-1 regulates c-Jun by assembling a CUL4A ubiquitin ligase, Science 303 (2004) 1371–1374.
[21] V. Rapic-Otrin, M.P. McLenigan, D.C. Bisi, M. Gonzalez, A.S. Levine, Sequential binding of UV DNA damage binding factor and degradation of the p48 subunit as early events after UV irradiation, Nucleic Acids Res. 30 (2002) 2588–2598.
[22] M.E. Fitch, I.V. Cross, S.J. Turner, S. Adimoolam, C.X. Lin, K.G. Williams, J.M. Ford, The DDB2 nucleotide excision repair gene product p48 enhances global genomic repair in p53 deficient human fibroblasts, DNA Repair 2 (2003) 819–826.

[23] T. Natsume, Y. Yamauchi, H. Nakayama, T. Shinkawa, M. Yanagida, N. Takahashi, T. Isobe, A direct nanoflow liquid chromatography-tandem mass spectrometry system for interaction proteomics, Anal. Chem. 74 (2002) 4725–4733.

[24] M. Komatsu, T. Chiba, K. Tatsumi, S.-I. Iemura, I. Tanida, N. Okazaki, T. Ueno, E. Kominami, T. Natsume, K. Tanaka, A novel protein-conjugating system for Ufm1, a ubiquitin-fold modifier, EMBO J. 23 (2004) 1977–1986.

[25] S. Handeli, H. Weintraub, The ts41 mutation in Chinese hamster cells leads to successive S phases in the absence of intervening G2, M, and G1, Cell 71 (1992) 599–611.

[26] N. Matsuda, T. Suzuki, K. Tanaka, A. Nakano, Rma1, a novel type of RING finger protein conserved from Arabidopsis to human, is a membrane-bound ubiquitin ligase, J. Cell Sci. 114 (2001) 1949–1957.

[27] N. Imai, N. Matsuda, K. Tanaka, A. Nakano, S. Matsumoto, W. Kang, Ubiquitin ligase activities of Bombyx mori nucleopolyhedrovirus RING finger proteins, J. Virol. 77 (2003) 923–930.

[28] L.C. Chen, S. Manjeshwar, Y. Lu, D. Moore, B.M. Ljung, W.L. Kuo, S.H. Dairkee, M. Wernick, C. Collins, H.S. Smith, The human homologue for the *Caenorhabditis elegans* cul-4 gene is amplified and overexpressed in primary breast cancers, Cancer Res. 58 (1998) 3677–3683.

[29] P. Shiyanov, S.A. Hayes, M. Donepudi, A.F. Nichols, S. Linn, B.L. Slagle, P. Raychaudhuri, The naturally occurring mutants of DDB are impaired in stimulating nuclear import of the p125 subunit and E2F1-activated transcription, Mol. Cell. Biol. 19 (1999) 4935–4943.

[30] V. Rapic-Otrin, M. McLenigan, M. Takao, A.S. Levine, M. Protic, Translocation of a UV-damaged DNA binding protein into a tight association with chromatin after treatment of mammalian cells with UV light, J. Cell Sci. 110 (1997) 1159–1168.

[31] W. Liu, A.F. Nichols, J.A. Graham, R. Dualan, A. Abbas, S. Linn, Nuclear transport of human DDB protein induced by ultraviolet light, J. Biol. Chem. 275 (2000) 21429–21434.

[32] B.J. Hwang, J.M. Ford, P.C. Hanawalt, G. Chu, Expression of the p48 xeroderma pigmentosum gene is p53-dependent and is involved in global genomic repair, Proc. Natl. Acad. Sci. U.S.A. 96 (1999) 424–428.

[33] T. Itoh, C. O'Shea, S. Linn, Impaired regulation of tumor suppressor p53 caused by mutations in the xeroderma pigmentosum DDB2 gene: mutual regulatory interactions between p48(DDB2) and p53, Mol. Cell. Biol. 23 (2003) 7540–7553.

[34] S. Keeney, H. Wein, S. Linn, Biochemical heterogeneity in xeroderma pigmentosum complementation group E, Mutat. Res. 273 (1992) 49–56.

[35] M. Araki, C. Masutani, T. Maekawa, Y. Watanabe, A. Yamada, R. Kusumoto, D. Sakai, K. Sugasawa, Y. Ohkuma, F. Hanaoka, Reconstitution of damage DNA excision reaction from SV40 minichromosomes with purified nucleotide excision repair proteins, Mutat. Res. 459 (2000) 147–160.

[36] S.J. Araujo, F. Tirode, F. Coin, H. Pospiech, J.E. Syvaoja, M. Stucki, U. Hubscher, J.M. Egly, R.D. Wood, Nucleotide excision repair of DNA with recombinant human proteins: definition of the minimal set of factors, active forms of TFIIH, and modulation by CAK, Genes Dev. 14 (2000) 349–359.

[37] D. Mu, C.H. Park, T. Matsunaga, D.S. Hsu, J.T. Reardon, A. Sancar, Reconstitution of human DNA repair excision nuclease in a highly defined system, J. Biol. Chem. 270 (1995) 2415–2418.

[38] A. Aboussekhra, M. Biggerstaff, M.K. Shivji, J.A. Vilpo, V. Moncollin, V.N. Podust, M. Protic, U. Hubscher, J.M. Egly, R.D. Wood, Mammalian DNA nucleotide excision repair reconstituted with purified protein components, Cell 80 (1995) 859–868.

[39] M. Wakasugi, M. Shimizu, H. Morioka, S. Linn, O. Nikaido, T. Matsunaga, Damaged DNA-binding protein DDB stimulates the excision of cyclobutane pyrimidine dimers in vitro in concert with XPA and replication protein A, J. Biol. Chem. 276 (2001) 15434–15440.

[40] M. Wakasugi, A. Kawashima, H. Morioka, S. Linn, A. Sancar, T. Mori, O. Nikaido, T. Matsunaga, DDB accumulates at DNA damage sites immediately after UV irradiation and directly stimulates nucleotide excision repair, J. Biol. Chem. 277 (2002) 1637–1640.

[41] Y. Yanagawa, J.A. Sullivan, S. Komatsu, G. Gusmaroli, G. Suzuki, J. Yin, T. Ishibashi, Y. Saijo, V. Rubio, S. Kimura, J. Wang, X.W. Deng, Arabidopsis COP10 forms a complex with DDB1 and DET1 in vivo and enhances the activity of ubiquitin conjugating enzymes, Genes Dev. 18 (2004) 2172–2181.

[42] L.A. Higa, I.S. Mihaylov, D.P. Banks, J. Zheng, H. Zhang, Radiation-mediated proteolysis of CDT1 by CUL4-ROC1 and CSN complexes constitutes a new checkpoint, Nat. Cell Biol. 5 (2003) 1008–1015.

[43] J. Hu, C.M. McCall, T. Ohta, Y. Xiong, Targeted ubiquitination of CDT1 by the DDB1–CUL4A-ROC1 ligase in response to DNA damage, Nat. Cell Biol. 6 (2004) 1003–1009.

[44] J.D. Schnell, L. Hicke, Non-traditional functions of ubiquitin and ubiquitin-binding proteins, J. Biol. Chem. 278 (2003) 35857–35860.

EMBO
reports

scientific report

Glycoprotein-specific ubiquitin ligases recognize *N*-glycans in unfolded substrates

Yukiko Yoshida[1,2+], *Eru Adachi*[1,2], *Kanako Fukiya*[1,2], *Kazuhiro Iwai*[2,3] & *Keiji Tanaka*[1]

[1]Tokyo Metropolitan Institute of Medical Science, Bunkyo-ku, Tokyo, Japan, [2]CREST, Japan Science and Technology Corporation (JST), Saitama, Japan, and [3]Department of Molecular Cell Biology, Graduate School of Medicine, Osaka City University, Osaka, Japan

Misfolded or unassembled polypeptides in the endoplasmic reticulum (ER) are retro-translocated into the cytosol and degraded by the ubiquitin–proteasome system. We reported previously that the $SCF^{Fbs1,2}$ ubiquitin-ligase complexes that contribute to ubiquitination of glycoproteins are involved in the ER-associated degradation pathway. Here we investigated how the $SCF^{Fbs1,2}$ complexes interact with unfolded glycoproteins. The SCF^{Fbs1} complex was associated with p97/VCP AAA ATPase and bound to integrin-β1, one of the SCF^{Fbs1} substrates, in the cytosol in a manner dependent on p97 ATPase activity. Both Fbs1 and Fbs2 proteins interacted with denatured glycoproteins, which were modified with not only high-mannose but also complex-type oligosaccharides, more efficiently than native proteins. Given that Fbs proteins interact with innermost chitobiose in *N*-glycans, we propose that Fbs proteins distinguish native from unfolded glycoproteins by sensing the exposed chitobiose structure.

Keywords: ubiquitin ligase; glycoprotein; unfold; *N*-glycan

EMBO reports (2005) 6, 239–244. doi:10.1038/sj.embor.7400351

INTRODUCTION

Most secretory and membrane proteins are co-translationally translocated into the lumen of the endoplasmic reticulum (ER). In the ER, these proteins are modified by *N*-linked oligosaccharides and subjected to 'quality control' in which aberrant proteins are distinguished from properly folded proteins (Ellgaard & Helenius, 2003). When the improperly folded or incompletely assembled proteins fail to restore their functional states, they are degraded by the ER-associated degradation (ERAD) system, which involves retrograde transfer of proteins from the ER to the cytosol followed by degradation by the proteasome. p97/VCP, a cytosolic ATPase member of the AAA ATPase family, may have several roles in the ERAD pathway. It has been suggested that the p97–Ufd1–Npl4 complex is required for the extraction of misfolded proteins from the ER into the cytosol (Tsai *et al*, 2002). Such a retro-translocation step would most probably be mediated by dual recognition of the substrates by p97, with the complex binding both the nonubiquitinated segment of a substrate and the attached polyubiquitin chain (Ye *et al*, 2003). The p97 complex, which associates with the ER membrane proteins VIMP and Derlin-1 through the amino-terminal domain of p97, is thought to be required for the extraction of misfolded proteins from the ER (Lilley & Ploegh, 2004; Ye *et al*, 2004). However, p97 has also been proposed to be important for the release of ERAD substrates after their export from the ER, and thereby for their accessibility to the proteasome (Elkabetz *et al*, 2004). The role of each of these functions remains to be established.

In the ubiquitin system, the ubiquitin ligase 'E3' has an important role in the selection of target proteins for ubiquitination. At present, several E3s have been identified in the ERAD pathway, such as Hrd1 (Bays *et al*, 2001) and Doa10 (Swanson *et al*, 2001) in yeast, and gp78 (Fang *et al*, 2001), CHIP (Meacham *et al*, 2001) and Parkin (Imai *et al*, 2001) in mammals. In addition, we have recently identified a new member of the ERAD-linked E3 family, SCF^{Fbs}, which participates in ERAD for selective elimination of glycoproteins (Yoshida *et al*, 2002, 2003). Whereas Hrd1, Doa10 and gp78 are localized in the ER, SCF^{Fbs} complexes are localized in the cytosol similar to CHIP and Parkin.

The SCF is composed of Cullin1/Cdc53, Skp1, Roc1/Rbx1, and one member of the large family of F-box proteins, which are involved in trapping target proteins (Deshaies, 1999). Fbs1 and Fbs2 (F-box protein that recognizes sugar chains) interact with glycoproteins containing high-mannose oligosaccharides, protein modification of which occurs in the ER. Our recent X-ray crystallographic and nuclear magnetic resonance (NMR) studies of the substrate-binding domain of Fbs1 have shown that Fbs1 recognizes the inner chitobiose of high-mannose oligosaccharides by a small hydrophobic pocket located at the top of the β-barrel (Mizushima *et al*, 2004).

In this study, we examined whether Fbs proteins discriminate between folded and unfolded glycoproteins because ERAD substrates are thought to be unfolded. Both Fbs1 and Fbs2 preferably bind to denatured proteins that contain not only

[1]Tokyo Metropolitan Institute of Medical Science, 3-18-22, Hon-komagome, Bunkyo-ku, Tokyo 113-8613, Japan
[2]CREST, Japan Science and Technology Corporation (JST), Saitama 332-0012, Japan
[3]Department of Molecular Cell Biology, Graduate School of Medicine, Osaka City University, Osaka 545-8585, Japan
+Corresponding author. Tel: +81 3 3823 2105; Fax: +81 3 3823 2965;
E-mail: yyosida@rinshoken.or.jp

Received 16 August 2004; revised 11 January 2005; accepted 13 January 2005; published online 18 February 2005

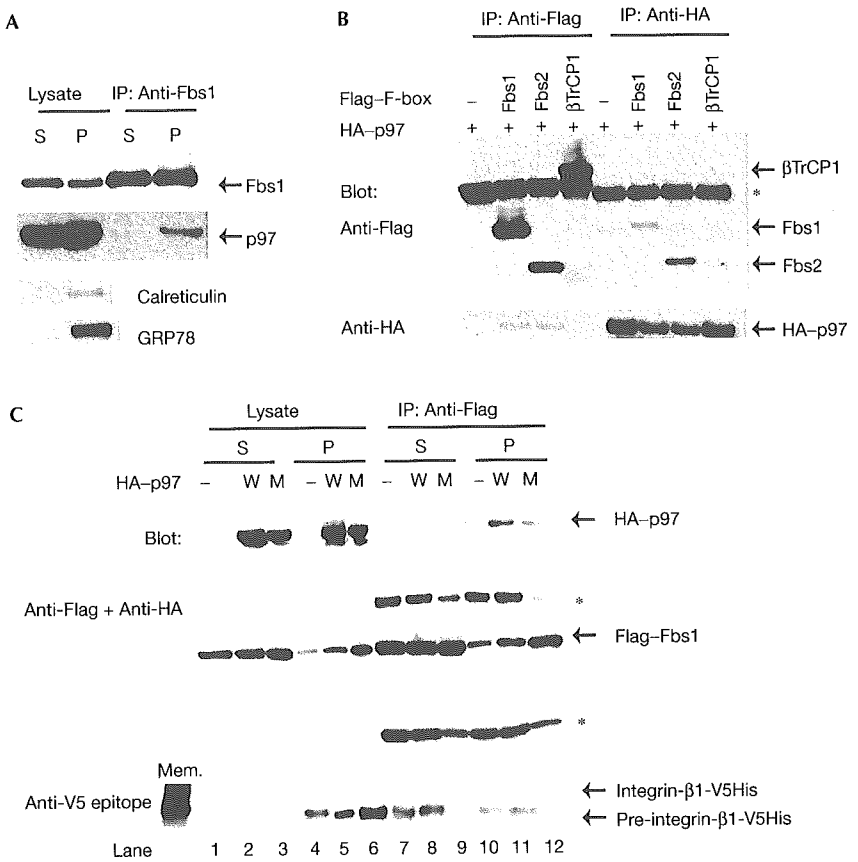

Fig 1 | Fbs1 binds to integrin-β1 dependent on p97 ATPase activity. (**A**) Fbs1 associates with p97 in microsomal fraction. Endogenous Fbs1 was immunoprecipitated from 100,000*g* supernatant (S) and precipitate (P) fractions of brains of adult mice. Lysate (15 μg each) and immunoprecipitates were analysed by immunoblotting with antibodies against Fbs1, p97, calreticulin and GRP78. (**B**) Interaction of Fbs proteins with p97. Lysates of 293T cells transiently expressing Flag-tagged F-box proteins (−, empty vector) and HA-tagged p97 were subjected to immunoprecipitation, and the resulting precipitates were analysed by immunoblotting. The asterisk shows immunoglobulin heavy chains. (**C**) Fbs1 binding to integrin-β1 in the cytosol depends on p97 ATPase activity. 293T cells were transfected with Flag-tagged Fbs1, V5-tagged integrin-β1 and HA-tagged p97 (−, empty vector; W, wild-type p97; M, mutant p97 (K524A)). Fbs1 was immunoprecipitated from supernatant (S) and precipitate (P) fractions. Expressions of p97, Fbs1 and integrin-β1 in fractionated lysates (5 μg each) and the amount of integrin-β1 associated with Fbs1 were analysed by immunoblotting using anti-V5 antibody. The membranous fraction (Mem.) was prepared from 24,000*g* precipitate. Asterisks show immunoglobulin heavy and light chains.

high-mannose but also complex-type oligosaccharides over native counterparts. The results showed that these F-box proteins probably interact with the innermost chitobiose in *N*-glycans in only unfolded glycoprotein in the ERAD pathway, considering that chitobiose moieties are usually masked by the folded polypeptide.

RESULTS

SCF^{Fbs} associates with the p97 complex

We have isolated Fbs1 from mouse brain cytosol as a novel sugar-binding protein that functions as a substrate-binding subunit in SCF-type E3 for ERAD (Yoshida *et al*, 2002), but the ubiquitination machinery for ERAD is probably associated with the ER membrane. To test the localization of Fbs1 proteins in mouse brain, we prepared anti-Fbs1 polyclonal antibodies. Lysates from adult mouse brain were fractionated into 100,000*g* supernatant (S) and precipitate (P) fractions excluding 24,000*g* precipitate, and the presence of Fbs1 was analysed by immunoblotting (Fig 1A). Fbs1 was detected in the P as well as the S fractions, suggesting that Fbs1 interacts with proteins that associate with the ER membrane. As p97/VCP is thought to be involved in the retro-transport of ERAD substrates (Tsai *et al*, 2002), we examined the interaction of Fbs1 with p97. As shown in Fig 1A, Fbs1 was co-immunoprecipitated with p97 from the P but not from the S fraction. To determine whether other F-box proteins interact with p97, the Flag-tagged F-box proteins were expressed, together with haemagglutinin (HA)-tagged p97, in 293T cells, immunoprecipitated and analysed by immunoblotting (Fig 1B). Both Fbs1 and Fbs2 but not βTrCP1, an F-box protein with WD repeats for substrate recognition, were co-immunoprecipitated with p97. These results suggest that a part of Fbs proteins binds specifically to the p97-containing complex at the ER.

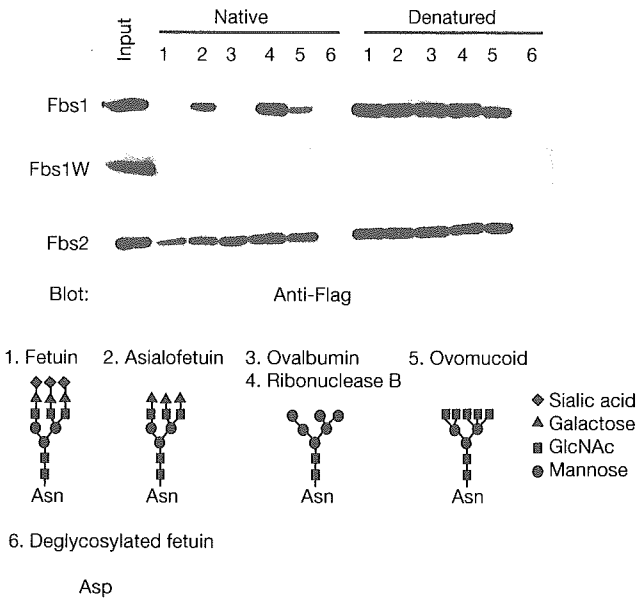

Fig 2 | Pull-down analysis of the interactions of Fbs1, Fbs1W and Fbs2 with native and denatured *N*-glycoproteins. Extracts of cells expressing Flag-tagged Fbs1, the W280A mutant of Fbs1 (Fbs1W) and Fbs2 were incubated with native or guanidine-HCl-treated (denatured) glycoproteins (lanes 1–5) or deglycosylated fetuin (lane 6)-immobilized beads. The beads were washed and then boiled with sample buffer. Lysates (7.5 μg) and bound proteins were analysed by immunoblotting using anti-Flag antibody (top) and the structures of *N*-glycans in the glycoproteins tested are shown at the bottom.

Fbs1 binds to integrin-β1 dependent on p97 activity

We identified pre-integrin-β1, which was modified with high-mannose oligosaccharides, as one of the Fbs1 substrates (Yoshida *et al*, 2002). As the Fbs1–pre-integrin-β1 interaction occurs in the cytosol, retro-translocation of integrin-β1 from the ER into the cytosol is required for Fbs1 binding. To analyse the involvement of p97 in the interaction between Fbs1 and pre-integrin-β1, 293T cells were transfected with expression plasmids encoding Flag-tagged Fbs1, V5-tagged integrin-β1 together with HA-tagged p97 or its mutant, and treated with the proteasome inhibitor MG132 for 1.5 h before collecting cells. Immunoprecipitates with anti-Flag antibody of S and P fractions of transfected 293T cells were immunoblotted with anti-V5 antibody to detect co-immunoprecipitated integrin-β1 (Fig 1C). Most of pre-integrin-β1 was localized in the P fractions, and the expression of the ATPase-defective p97 mutant (K524A) increased the amount of total pre-integrin-β1 in the P fraction (lanes 4–6). The amount of pre-integrin-β1 associated with Fbs1 was greater in wild-type p97-expressing cells than in mutant p97-expressing cells in both S and P fractions (lanes 7–12). These results suggest that Fbs proteins recognize and ubiquitinate pre-integrin-β1 retro-translocated by p97, and this modification may facilitate pre-intergrin-β1 binding to the p97–Ufd1–Npl4 complex, as well as its extraction from the ER.

Fbs interacts with denatured *N*-glycoproteins

Glycoproteins retro-translocated from the ER are not native proteins. Therefore, to examine whether Fbs proteins recognize denatured glycoproteins better than native proteins, first we carried out a pull-down assay using several *N*-glycoproteins (Fig 2). We have reported that both Fbs1 and Fbs2 recognize the innermost chitobiose structure in high-mannose oligosaccharides (Yoshida *et al*, 2003). Although both ovalbumin and ribonuclease B (RNaseB) contain high-mannose oligosaccharides, Fbs1 effectively bound to RNaseB alone (see Discussion). Fbs1 could bind to asialofetuin and ovomucoid, but could hardly bind to fetuin and ovalbumin. The ability of Fbs2 to bind to asialofetuin, fetuin and ovomucoid was weaker than that to proteins attached to the high-mannose oligosaccharides. Interestingly, both Fbs proteins could bind to all the denatured *N*-glycoproteins tested but not to denatured deglycosylated proteins (lane 6), whereas the W280A mutant of Fbs1 (Fbs1W) that fails to interact with the innermost GlcNAc moiety in *N*-glycan (Mizushima *et al*, 2004) could not bind to any native or denatured glycoproteins, suggesting that the denaturation of glycoproteins increases the accessibility to the innermost chitobiose of *N*-glycans by Fbs proteins.

We next examined whether the binding potency and substrate specificity of Fbs proteins are influenced by denaturation of cellular glycoproteins. Lysates from the mouse brain or Neuro2a cells were treated with or without 6 M guanidine-HCl, diluted ten times with the lysis buffer and incubated with the His-tagged Fbs proteins produced by *Escherichia coli* (Fig 3; supplementary information 1 online). Guanidine-HCl at 0.6 M had no influence on Fbs binding to glycoproteins (supplementary information 2 online). The glycoproteins bound to Fbs were isolated using Ni-NTA affinity chromatography and detected by lectin blotting (Fig 3). Blotting with GNA, a lectin that binds to high-mannose oligosaccharide, showed that denaturation markedly increased the number of proteins bound to Fbs. The spectrum of Fbs1-bound protein bands in the brain detected by WGA, a lectin specific for terminal GlcNAc or sialic acids, was similar to those detected by GNA, suggesting that these proteins are modified by both high-mannose and complex-type oligosaccharides. Conversely, the proteins detected by RCA120, a lectin that binds to terminal galactose-β1-4GlcNAc, were different to those detected by GNA. Both the quantities and species of RCA120-reactive proteins recognized by Fbs1 were also considerably increased by denaturation. Treatment of denatured proteins with peptide:*N*-glycanase (PNGase F) almost diminished their binding to Fbs. Furthermore, Fbs1W could hardly bind these glycoproteins. These results strongly suggest that both Fbs1 and Fbs2 bind to the innermost GlcNAc moiety irrespective of the terminal sugar moieties, and that the accessibility of Fbs proteins to the innermost GlcNAc moiety is enhanced by denaturation of the substrate glycoproteins. As all *N*-linked oligosaccharides contain innermost chitobiose structure, Fbs proteins seem to be capable of binding most *N*-glycoproteins when denatured.

SCF^{Fbs1} ubiquitinates denatured glycoproteins

To see whether SCF^{Fbs} ubiquitinates denatured glycoproteins more efficiently than native counterparts, we performed an *in vitro* ubiquitination assay using purified components including recombinant SCF^{Fbs1} proteins. Efficient ubiquitination of GlcNAc-terminated fetuin (GTF), which is an *in vitro* substrate for SCF^{Fbs1} (Yoshida *et al*, 2002), was detected by immunoblotting using an anti-fetuin antibody. When an excess amount of substrates existed, denatured asialofetuin was efficiently ubiquitinated,

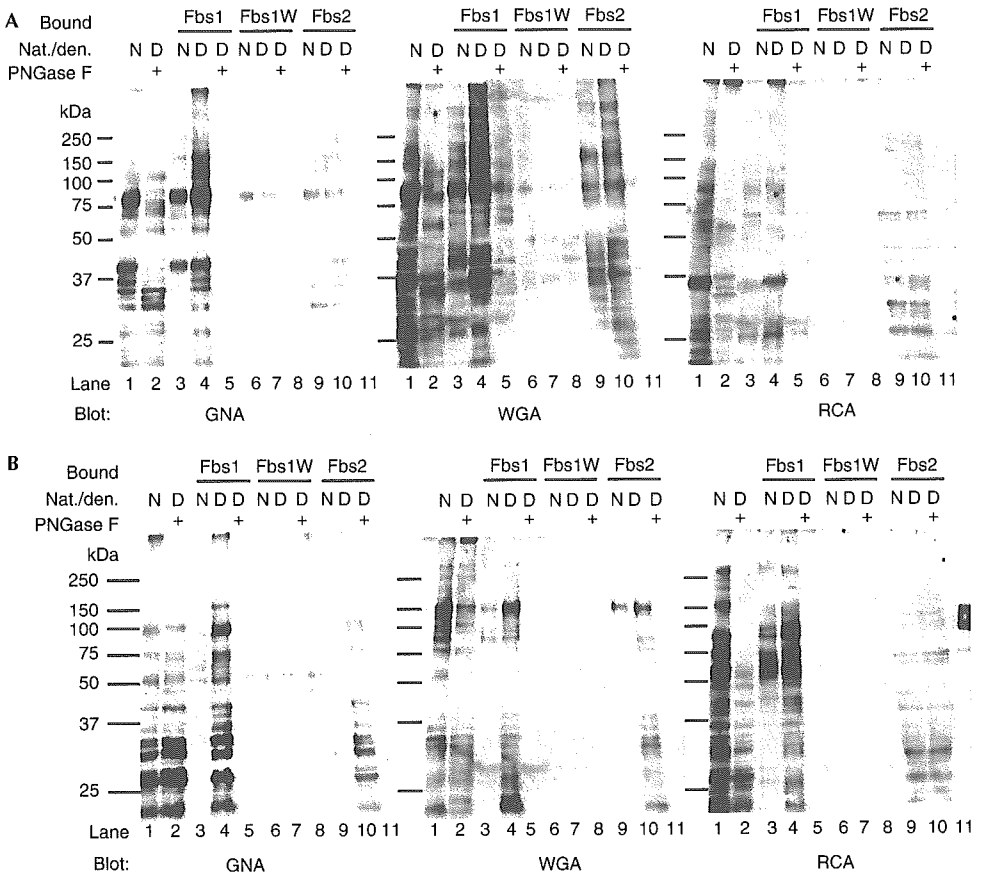

Fig 3 | Interactions of Fbs1 and Fbs2 with cellular glycoproteins containing *N*-linked oligosaccharides in native and denatured states. Native (N), denatured (D) or PNGase-treated proteins prepared form mouse brain (**A**) or Neuro2a cells (**B**) were incubated with recombinant Fbs1-, Fbs1W- and Fbs2-immobilized beads. Native and PNGase-treated lysates (15 μg each; lanes 1 and 2) and proteins bound to Fbs1, Fbs1W or Fbs2 were analysed by lectin blotting using HRP-labelled GNA, WGA and RCA.

whereas ubiquitination of native asialofetuin was marginal (Fig 4; supplementary information 3 online). No ubiquitination of GTF or denatured asialofetuin was detected in the absence of E1, E2, ATP or substrate, and SCF^{Fbs1W} (Mizushima *et al*, 2004) failed to ubiquitinate these substrates (supplementary information 4 online). These results demonstrate that the higher affinity of Fbs1 for denatured *N*-glycoproteins results in a more efficient ubiquitination of the denatured substrates than native counterparts.

DISCUSSION

In the early secretory pathway, *N*-glycosylation facilitates conformational maturation by promoting the glycoprotein-folding machinery, and functions as tags for ER retention and targeting to the ERAD pathway. The calnexin–calreticulin cycle, consisting of two homologous lectins, calnexin and calreticulin, which interact with monoglucosylated *N*-glycans, in concert with UDP-glucose:glycoprotein glucosyltransferase (GT) and glucosidase II, has a central role in folding and ER retention. Conversely, it is shown that α-mannosidase I and EDEM have a pivotal role in selective disposal of misfolded glycoproteins (Ellgaard & Helenius, 2003; Yoshida, 2003). Among these oligosaccharide-related molecules in the ER, only GT has been shown to recognize incompletely folded proteins (Parodi, 2000). In the cytosol, the *N*-glycans in proteins extracted from the ER are removed before proteolysis by PNGase. In addition, PNGase can discriminate between non-native and folded glycoproteins, favouring the former (Hirsch *et al*, 2004). In this study, we showed that the Fbs proteins preferentially bind to denatured glycoproteins over properly folded proteins. As the retro-translocated proteins in the cytosol from the ER are misfolded, it is conceivable that *N*-glycan recognition proteins in the cytosol can sense misfolded states.

Although GT and PNGase can distinguish the folding states of substrates, the structural elements required for identification of their targets are not fully understood. *In vitro* studies have shown that GT also preferentially re-glucosylates glycoproteins in partially folded, molten globule conformations (Caramelo *et al*, 2003), and that an important feature for recognition is the exposure of hydrophobic clusters and innermost GlcNAc residue (Sousa & Parodi, 1995). Fbs1 interacts with the inner chitobiose in *N*-glycans of glycoproteins by a specific binding surface located at one tip of the β-sandwich of its substrate-binding domain (Mizushima *et al*, 2004). The intramolecular interactions of

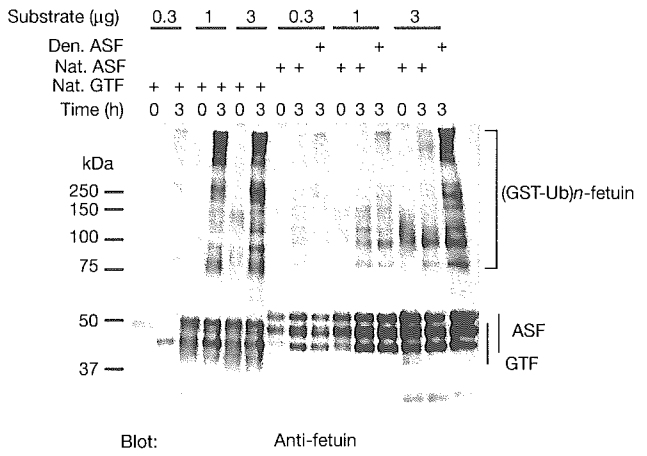

Fig 4 | *In vitro* ubiquitination of native GlcNAc-terminated fetuin (GTF), asialofetuin (ASF) and denatured ASF by SCF^{Fbs1} ligase. The high-molecular-mass ubiquitinated fetuin ((GST-Ub)*n*-fetuin) was detected by immunoblotting with anti-fetuin antibody.

innermost GlcNAc residue and the polypeptide moiety generally hamper the binding of Fbs1 to the chitobiose portions of glycoproteins as a result of steric hindrance in their native states. Therefore, Fbs1 recognizes the innermost position of *N*-glycans as a signal for unfolded glycoproteins. Conversely, as RNaseB contains an oligosaccharide that does not contact the polypeptide chain except at the covalent attachment point (Williams *et al*, 1987), it is likely that RNaseB interacts with Fbs1 even in the native form probably due to the exceptional freedom of the innermost chitobiose portion (Fig 2). The present results confirmed that Fbs proteins bind to denatured glycoproteins.

Considering that ubiquitination of ERAD substrates is linked to retro-translocation and rapid degradation, ubiquitin ligases for ERAD might be associated with the ER membrane. Moreover, as many glycoproteins are efficiently deglycosylated by PNGase after retrograde transfer into the cytosol (Blom *et al*, 2004), the rapid recognition of substrate by Fbs proteins before deglycosylation is critical. We found a part of Fbs proteins in association with p97 in the microsomal fractions, and extraction of the substrate of SCF^{Fbs1} was dependent on the ATPase activity of p97 followed by association with Fbs1. Thus, SCF^{Fbs} seems to be positioned in the ER membrane in such a way that it can ubiquitinate substrates immediately after retro-translocation to the cytosol.

Fbs proteins can bind not only high-mannose oligosaccharides but also various types of *N*-glycans in glycoproteins. These modified glycoproteins other than the high-mannose oligosaccharides are not ERAD substrates. Therefore, our finding suggests that SCF^{Fbs} mediates ubiquitination of exogenous or membrane proteins endocytosed into the cells. This is not unusual, because it is well known that extracellular proteins incorporated by phagocytosis into dendritic cells are presented to MHC class I molecules after proteasomal degradation (Castellino *et al*, 2000). Other studies demonstrated the transfer of endocytosed proteins into the cytosol by unknown mechanisms before their proteasomal processing and/or destruction (Kovacsovics-Bankowski & Rock, 1995). Further functional analysis of Fbs family proteins can shed light on the degradation of endocytosed proteins.

METHODS

Transfection, plasmids, antibodies, immunoprecipitation and immunoblotting. 293T cells were transfected as described previously (Yoshida *et al*, 2002). HA–p97-expressing plasmid was a kind gift from S. Khochbin (INSERM, France). HA–p97 (K524A)-expressing plasmid was constructed by site-directed mutagenesis. Human integrin-β1 complementary DNA was cloned from cDNA clone (ATCC 988953) in pTracer-EF-V5His vector (Invitrogen, Carlsbad, CA, USA). The anti-mouse Fbs1 serum was generated in rabbits by standard procedures using a synthetic peptide corresponding to residues 1–14 (MDGDGDPFSVSHPE) of the predicted protein coupled to keyhole limpet haemocyanin. Monoclonal antibodies to p97 and V5 epitope were purchased from Progen (Heidelberg, Germany) and Invitrogen, respectively, and polyclonal antibodies to calreticulin and GRP78 were from Affinity Bioreagents (Exeter, Devon, UK). Antibodies to Flag, HA and fetuin have been described previously (Yoshida *et al*, 2003). Immunoprecipitation from whole-cell extracts or subcellular fractionation of cells and immunoblotting were performed in TBS-T (1% Triton X-100, 50 mM Tris–HCl pH 7.5, 150 mM NaCl and protease inhibitors) as described previously (Yoshida *et al*, 2002).

Pull-down assay. Fetuin, asialofetuin, ovalbumin, RNaseB and ovomucoid were purchased from Sigma-Aldrich (St Louis, MO, USA). For preparation of deglycosylated fetuin (DGF), 10 mg of asialofetuin was incubated with 200 U of PNGase F (Roche, Mannheim, Germany) in 50 mM phosphate buffer, pH 7.2, at 37 °C for 24 h. The enzyme-treated proteins were loaded onto successive WGA and RCA-lectin agarose columns. The flow-through fraction from both columns was used as DGF. Each 10 mg glycoprotein was immobilized to 0.5 ml of Affi-gel 10 or 15 (Bio-Rad, Richmond, CA, USA). For preparation of denatured-glycoprotein-immobilized beads, after each half of glycoprotein-immobilized beads was incubated in 6 M guanidine-HCl for 2 h, the beads were washed five times with ten volumes of 20 mM Tris–HCl (pH 7.5)/150 mM NaCl (TBS) containing 0.5% NP-40 (TBS-N). Each cell extract prepared with TBS-N from Flag-tagged Fbs1, Fbs1 W280A mutant or Fbs2-expressing 293T cells (30 μg) was incubated with 15 μl of various glycoprotein-immobilized beads. Bound proteins were eluted by boiling with SDS sample buffer and were analysed by immunoblotting.

Binding assay and lectin blotting. The substrate-binding domain of mouse Fbs1 (117–297) and its W280A mutant were cloned into pET15b (Mizushima *et al*, 2004), that of mouse Fbs2 (46–295) was cloned into pET33b, and expressed in *E. coli*. The His-tagged Fbs proteins were bound to Ni-NTA agarose beads (Qiagen, Hilden, Germany). Mouse brains and Neuro2a cells were homogenized in TBS-N and protease inhibitors. After centrifugation of the homogenate at 15,000*g* for 30 min, guanidine-HCl was dissolved with one-third of the supernatant (protein concentration 5 mg ml^{-1}) up to 6 M. Guanidine-HCl-treated and untreated lysates were diluted ten times with TBS-N. Another aliquot was treated with PNGase F subsequent to denaturation by heating for 5 min at 100 °C in the presence of 1% SDS and was then diluted ten times with TBS-N. The dilutes and PNGase-treated lysates were precleared with Ni-NTA agarose and then the flow-through fractions were incubated with the Fbs-protein-bound beads for 18 h at 4 °C. The beads were washed with TBS-N containing 20 mM imidazole. The adsorbed proteins were eluted by 0.2 M

imidazole in TBS-N. Eluted proteins were separated by SDS–PAGE, and blotted onto a membrane (Immobilon). After the blotted membranes were blocked with 3% bovine serum albumin in PBS, lectin blotting was performed using horseradish peroxidase (HRP)-labelled GNA (EY Laboratories), RCA120 and WGA (Seikagaku-kogyo, Japan).

***In vitro* ubiquitination assays.** Preparation of GTF and *in vitro* ubiquitination assays were performed as described previously (Yoshida *et al*, 2002). Denatured asialofetuin was prepared by 200 times dilution of 20 mg ml^{-1} asialofetuin treated with 6 M guanidine-HCl. Details of the assay condition are described in supplementary information 5 online.

Supplementary information is available at *EMBO reports* online (http://www.emboreports.org).

ACKNOWLEDGEMENTS

We thank F. Tokunaga for helpful comments on the manuscript. This work was supported in part by Grants-in-Aid from the Ministry of Education, Science, Culture of Japan and the Hayashi Memorial Foundation for Female Natural Scientists, and the Seki Memorial Foundation for Science, Tokyo, Japan.

REFERENCES

Bays NW, Gardner RG, Seelig LP, Joazeiro CA, Hampton RY (2001) Hrd1p/Der3p is a membrane-anchored ubiquitin ligase required for ER-associated degradation. *Nat Cell Biol* **3:** 24–29

Blom D, Hirsch C, Stern P, Tortorella D, Ploegh HL (2004) A glycosylated type I membrane protein becomes cytosolic when peptide: *N*-glycanase is compromised. *EMBO J* **23:** 650–658

Caramelo JJ, Castro OA, Alonso LG, De Prat-Gay G, Parodi AJ (2003) UDP-Glc:glycoprotein glucosyltransferase recognizes structured and solvent accessible hydrophobic patches in molten globule-like folding intermediates. *Proc Natl Acad Sci USA* **100:** 86–91

Castellino F *et al* (2000) Receptor-mediated uptake of antigen/heat shock protein complexes results in major histocompatibility complex class I antigen presentation via two distinct processing pathways. *J Exp Med* **191:** 1957–1964

Deshaies RJ (1999) SCF and Cullin/Ring H2-based ubiquitin ligases. *Annu Rev Cell Dev Biol* **15:** 435–467

Elkabetz Y, Shapira I, Rabinovich E, Bar-Nun S (2004) Distinct steps in dislocation of luminal endoplasmic reticulum-associated degradation substrates: roles of endoplamic reticulum-bound p97/Cdc48p and proteasome. *J Biol Chem* **279:** 3980–3989

Ellgaard L, Helenius A (2003) Quality control in the endoplasmic reticulum. *Nat Rev Mol Cell Biol* **4:** 181–191

Fang S, Ferrone M, Yang C, Jensen JP, Tiwari S, Weissman AM (2001) The tumour autocrine motility factor receptor, gp78, is a ubiquitin protein ligase implicated in degradation from the endoplasmic reticulum. *Proc Natl Acad Sci USA* **98:** 14422–14427

Hirsch C, Misaghi S, Blom D, Pacold ME, Ploegh HL (2004) Yeast *N*-glycanase distinguishes between native and non-native glycoproteins. *EMBO Rep* **5:** 201–206

Imai Y, Soda M, Inoue H, Hattori N, Mizuno Y, Takahashi R (2001) An unfolded putative transmembrane polypeptide, which can lead to endoplasmic reticulum stress, is a substrate of Parkin. *Cell* **105:** 891–902

Kovacsovics-Bankowski M, Rock KL (1995) A phagosome-to-cytosol pathway for exogenous antigens presented on MHC class I molecules. *Science* **267:** 243–246

Lilley BN, Ploegh HL (2004) A membrane protein required for dislocation of misfolded proteins from the ER. *Nature* **429:** 834–840

Meacham GC, Patterson C, Zhang W, Younger JM, Cyr DM (2001) The Hsc70 co-chaperone CHIP targets immature CFTR for proteasomal degradation. *Nat Cell Biol* **3:** 100–105

Mizushima T *et al* (2004) Structural basis of sugar-recognizing ubiquitin ligase. *Nat Struct Mol Biol* **11:** 365–370

Parodi AJ (2000) Protein glucosylation and its role in protein folding. *Annu Rev Biochem* **69:** 69–93

Sousa M, Parodi AJ (1995) The molecular basis for the recognition of misfolded glycoproteins by the UDP-Glc:glycoprotein glucosyltransferase. *EMBO J* **14:** 4196–4203

Swanson R, Locher M, Hochstrasser M (2001) A conserved ubiquitin ligase of the nuclear envelope/endoplasmic reticulum that functions in both ER-associated and Matα2 repressor degradation. *Genes Dev* **15:** 2660–2674

Tsai B, Ye Y, Rapoport TA (2002) Retro-translocation of proteins from the endoplasmic reticulum into the cytosol. *Nat Rev Mol Cell Biol* **3:** 246–255

Williams RL, Greene SM, McPherson A (1987) The crystal structure of ribonuclease B at 2.5-Å resolution. *J Biol Chem* **262:** 16020–16031

Ye Y, Meyer HH, Rapoport TA (2003) Function of the p97–Ufd1–Npl4 complex in retrotranslocation from the ER to the cytosol: dual recognition of nonubiquitinated polypeptide segments and polyubiquitin chains. *J Cell Biol* **162:** 71–84

Ye Y, Shibata Y, Yun C, Ron D, Rapoport TA (2004) A membrane protein complex mediates retro-translocation from the ER lumen into the cytosol. *Nature* **429:** 841–847

Yoshida Y (2003) A novel role for *N*-glycans in the ERAD system. *J Biochem, (Tokyo)* **134:** 183–190

Yoshida Y *et al* (2002) E3 ubiquitin ligase that recognizes sugar chains. *Nature* **418:** 438–442

Yoshida Y, Tokunaga F, Chiba T, Iwai K, Tanaka K, Tai T (2003) Fbs2 is a new member of the E3 ubiquitin ligase family that recognizes sugar chains. *J Biol Chem* **278:** 43877–43884

THE JOURNAL OF BIOLOGICAL CHEMISTRY
Vol. 280, No. 12, Issue of March 25, pp. 11635–11640, 2005
Printed in U.S.A.

Co-chaperone CHIP Associates with Expanded Polyglutamine Protein and Promotes Their Degradation by Proteasomes*

Received for publication, October 25, 2004, and in revised form, January 14, 2005
Published, JBC Papers in Press, January 21, 2005, DOI 10.1074/jbc.M412042200

Nihar Ranjan Jana‡§¶, Priyanka Dikshit‡¶, Anand Goswami‡, Svetlana Kotliarova‖, Shigeo Murata, Keiji Tanaka**, and Nobuyuki Nukina‖‡‡**

*From the ‡Cellular and Molecular Neuroscience Laboratory, National Brain Research Centre, Manesar, Gurgaon 122-050, India, the ‖Laboratory for Structural Neuropathology, RIKEN Brain Science Institute, 2-1 Hirosawa, Wako-shi, Saitama 351-0198, Japan, and the **Department of Molecular Oncology, Tokyo Metropoliton Institute of Medical Science, Bankyo-ku, Tokyo 113-8613, Japan*

A major hallmark of the polyglutamine diseases is the formation of neuronal intranuclear inclusions of the disease proteins that are ubiquitinated and often associated with various chaperones and proteasome components. But, how the polyglutamine proteins are ubiquitinated and degraded by the proteasomes are not known. Here, we demonstrate that CHIP (C terminus of Hsp70-interacting protein) co-immunoprecipitates with the polyglutamine-expanded huntingtin or ataxin-3 and associates with their aggregates. Transient overexpression of CHIP increases the ubiquitination and the rate of degradation of polyglutamine-expanded huntingtin or ataxin-3. Finally, we show that overexpression of CHIP suppresses the aggregation and cell death mediated by expanded polyglutamine proteins and the suppressive effect is more prominent when CHIP is overexpressed along with Hsc70.

The pathological expansion of unstable trinucleotide repeats has been found to cause 15 neurological diseases, 9 of which are neurodegenerative diseases (also referred to as polyglutamine diseases) resulting from the expansion of CAG repeats within the coding region of the responsible genes. Those nine include Huntington's disease (HD),[1] dentatorubral pallidoluysian atrophy, X-linked spinal bulbar muscular atrophy (SBMA), and several spinocerebellar ataxias (SCA1, SCA2, SCA3, SCA6, SCA7, and SCA17). All nine disorders are progressive, dominantly inherited (except spinal bulbar muscular atrophy), typically begin in midlife, and result in severe neuronal dysfunction and neuronal cell death. Increasing length of glutamine repeats in the affected individual strongly correlates with earlier age of onset and disease severity (1).

Evidence suggests a toxic gain-of-function effect of the polyglutamine expansion on the protein, and this novel neurotoxic property most likely involves an increased propensity for the disease protein to aggregate (2). In human disease tissue, transgenic animal models, and transfected cells expanded polyglutamine proteins have been shown to undergo intracellular aggregation, in most cases forming neuronal intranuclear inclusions (3). However, the discovery of ubiquitinated aggregates or the neuronal intranuclear inclusions and the association of various chaperones and proteasome components with the aggregates suggest that the cells recognize the aggregated disease protein as abnormal and may represent an appropriate cellular response to refold or degrade aggregated mutant protein (4–9). Consistent with this idea, it has been experimentally demonstrated that overexpression of selective chaperones in the mammalian cell culture suppresses the aggregate formation and cell death (4, 6, 7, 9) and that the proteasome system is indeed involved in the degradation of polyglutamine proteins (5, 10, 11). However, very little is known about the delivery of the expanded-polyglutamine proteins to the ubiquitin proteasome pathway (UPP) for degradation.

In the present investigation, we studied the detail mechanism of ubiquitination of the expanded polyglutamine proteins using polyglutamine-expanded truncated N-terminal huntingtin (tNhtt) as well as truncated ataxin-3 as models. We found that CHIP, an ubiquitin ligase, associates with the expanded polyglutamine proteins and is responsible for their ubiquitination and degradation by proteasomes.

EXPERIMENTAL PROCEDURES

Materials—Lactacystin, 3-(4,5-dimethylthiazol-2-yl)-2,5-diphenyltetrazolium bromide (MTT), dbcAMP, and all cell culture reagents were obtained from Sigma. Lipofectamine 2000, Zeocin, G418, ponasterone A, and mouse monoclonal anti-v5 were purchased from Invitrogen. Rabbit polyclonal anti-ubiquitin was from Dako, and mouse monoclonal anti-GFP was from Roche Applied Science. Goat anti-mouse IgG-Cy3 was purchased from Molecular Probes and horseradish peroxidase-conjugated anti-mouse and anti-rabbit IgG were from Amersham Biosciences.

Expression Plasmids and Stable Cell Lines—The enhanced green fluorescence protein (EGFP) and tNhtt expression constructs, pIND-tNhtt-EGFP-16Q, pIND-tNhtt-150Q, and the generation of the stable cell lines of these constructs have been described previously (12). The construction of plasmids, pEGFP-N1-MJD(f)-20CAG and pEGFP-N1-MJD(f)-130CAG, pEGFP-N1-MJD(t)-20CAG, and pEGFP-N1-MJD(t)-80CAG were described elsewhere (13). The full-length CHIP cDNA was isolated from the total RNA extracted from HeLa cells by reverse transcription-PCR. Construction of full-length and the U-box-deleted CHIP in pcDNA vector with v5 tag were made using PCR.

Cell Culture, Transfection, Cell Viability Assay, and Counting of Aggregates—The wild type mouse neuro2a cells were cultured in Dulbecco's modified Eagle's medium supplemented with 10% heat-inactivated fetal bovine serum and the antibiotics penicillin/streptomycin. The stable cell lines (HD 16Q and HD 150Q) were maintained in the

* This work was supported by a grant-in-aid from the Ministry of Health, Labor and Welfare, from the Ministry of Education, Culture, Sports, Science and Technology, Japan, and from the Department of Biotechnology, Government of India. The costs of publication of this article were defrayed in part by the payment of page charges. This article must therefore be hereby marked "*advertisement*" in accordance with 18 U.S.C. Section 1734 solely to indicate this fact.

§ To whom correspondence may be addressed. Tel.: 91-124-2338922; Fax: 91-124-2338927; E-mail: nihar@nbrc.ac.in.
¶ Both authors contributed equally to this work.
‡‡ To whom correspondence may be addressed. E-mail: nukina@riken.brain.go.jp.

[1] The abbreviations used are: HD, Huntington's disease; UPP, ubiquitin proteasome pathway; tNhtt; truncated N-terminal huntingtin; MTT, 3-(4,5-dimethylthiazol-2-yl)-2,5-diphenyltetrazolium bromide; dbcAMP, N^6,2′-*O*-dibutyryl-adenosine-3′:5′-cyclic monophosphate; GFP, green fluorescent protein; EGFP, enhanced GFP; HSC, heat shock cognate.

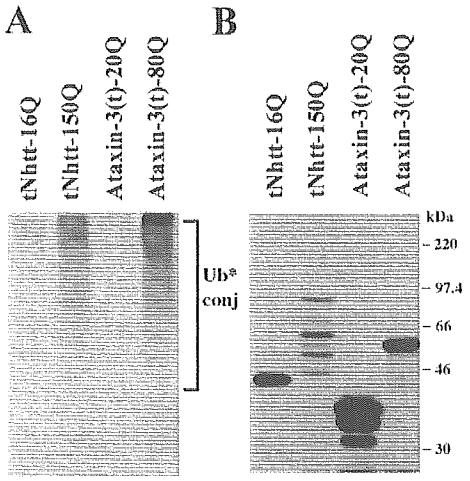

FIG. 1. **Ubiquitination of expanded polyglutamine proteins.** The HD 16Q and HD 150Q cell lines were induced with 1 μM ponasterone A, or the truncated ataxin-3-EGFP fusion constructs with 20Q and 80Q were transiently transfected (1 μg of each/well of 6-well tissue-cultured plate) to the neuro2a cells. Twenty-four hours after induction or transfection, cell lysate were made and subjected to immunoprecipitation as described under "Experimental Procedures." Blots were probed sequentially with ubiquitin antibody (*A*) and GFP antibody (*B*). *Ub * conj*, ubiquitin conjugates.

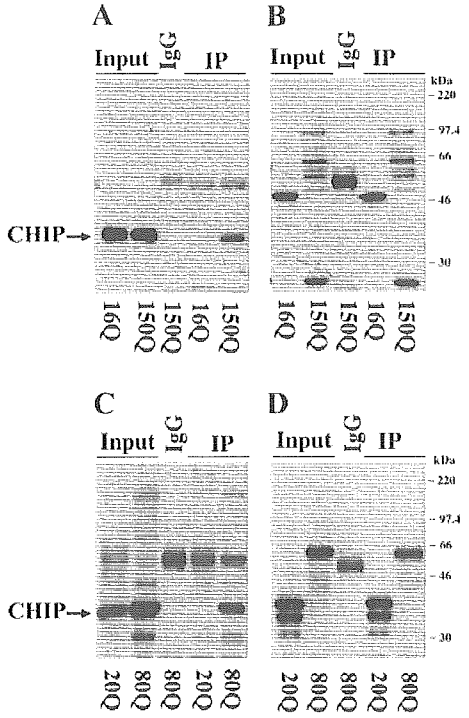

FIG. 2. **Interaction of CHIP with the expanded polyglutamine proteins.** *A* and *B*, the HD 16Q and HD 150Q cell lines were transiently transfected with CHIP (2 μg/well of 6-well tissue-cultured plate), and 12 h after transfection, media were changed, and the cells were induced with 1 μM ponasterone A. Twenty-four hours after induction, cells were collected and processed for immunoprecipitation (*IP*) by anti-GFP. Blots were sequentially probed with anti-v5 (*A*) and anti-GFP (*B*). *C* and *D*, neuro2a cells were first transfected with CHIP (2 μg/well of 6-well tissue-cultured plate). Twelve hours after first transfection, the medium was changed, and the cells were transfected again with the truncated ataxin-3-EGFP fusion constructs (1 μg of each/well) containing 20Q and 80Q. Twenty-four hours after the transfection of ataxin-3 constructs, cell lysates were made and subjected to immunoprecipitation as described in *A* and *B*. The blots were sequentially probed with anti-v5 (*C*) and anti-GFP (*D*).

same medium containing 0.4 mg/ml Zeocin and 0.4 mg/ml G418. One day prior to transfection, cells were plated into 6-well tissue-cultured plates at a subconfluent density. Cells were transiently transfected with expression vectors using Lipofectamine 2000 reagent according to the manufacturer's instruction. Transfection efficiency was ~80–90%. After 24 or 48 h of transfection, cells were used for immunofluorescence staining, co-immunoprecipitation, and immunoblotting. For cell viability assay, cells were first transfected with different expression plasmids. Twelve hours later, cells were harvested and replated into 96-well plates (5×10^3 cells/well). The cells were then differentiated with 5 mM dbcAMP and induced with 1 μM ponasterone A for 3 days. Cell viability was measured by MTT assay as described previously (12). Statistical analysis was performed using Student's t test, and $p < 0.05$ was considered to indicate statistical significance. Aggregate formation was manually counted under a fluorescence microscope (~500 transfected cells in each case), and the cells containing more than one aggregate were considered to have a single aggregate.

Co-immunoprecipitation and Immunoblotting Experiment—After 24 or 48 h of transfection, cells were washed with cold phosphate-buffered saline, scraped, pelleted by centrifugation, and lysed on ice for 30 min with radioimmune precipitation assay buffer (10 mM Hepes (pH 7.4), 150 mM NaCl, 10 mM EDTA, 2.5 mM EGTA, 1% Triton X-100, 0.1% SDS, 1% sodium deoxycholate, 10 mM NaF, 5 mM $Na_4P_2O_7$, 0.1 mM Na_2VO_5, 1 mM phenylmethylsulfonyl fluoride, 0.1 mg/ml Aprotinin). Cell lysates were briefly sonicated, centrifuged for 10 min at 15,000 $\times g$ at 4 °C, and the supernatants (total soluble extract) were used for immunoprecipitation as described earlier (9). For each immunoprecipitation experiment, 200 μg of protein in 0.2 ml of radioimmune precipitation assay buffer was incubated either with 5 μl (2 μg) of GFP antibody or 4 μl (2 μg) of normal mouse IgG. Bound proteins were eluted from the beads with SDS (1×) sample buffer, vortexed, boiled for 5 min, and analyzed by immunoblotting according to the procedure described earlier (9). Blot detection was carried out with enhanced chemiluminescence reagent. All primary antibodies were used in 1:1000 dilutions for immunoblotting.

Immunofluorescence Techniques—Cells grown in chamber slides or in 6-well tissue cultured plates were transiently transfected with different constructs. Forty-eight hours after transfection, cells were washed twice with phosphate-buffered saline, fixed with 4% paraformaldehyde in phosphate-buffered saline for 20 min, permeabilized with 0.5% Triton X-100 in phosphate-buffered saline for 5 min, washed extensively, then blocked with 5% nonfat dried milk in TBST (50 mM Tris, pH 7.5, 0.15 M NaCl, 0.05% Tween) for 1 h. Primary antibody (anti-v5, 1:5000 dilutions) incubation was carried out overnight at 4 °C. After several washings with TBST, cells were incubated with Cy3-conjugated secondary antibody (1:500 dilutions) for 1 h, washed several times, and mounted in antifade solution. Samples were observed using a confocal microscope (Fluoview, Olympus), and digital images were assembled using Adobe Photoshop.

Degradation Assay—Neuro2a cells were plated in a 6-well tissue-cultured plate, and on the following day, cells were transiently transfected with full-length ataxin-3 with 20Q and 130Q with or without CHIP. Twenty-four hours post-transfection, cells were chased with 10 μg/ml of cycloheximide for different time periods. Cells collected at each time point were then processed for immunoblotting by anti-GFP.

RESULTS

Misfolded Truncated N-terminal Huntingtin or Ataxin-3 Are Ubiquitinated—We developed several stable neuro2a cell lines in an inducible system, that express tNhtt with normal (16Q) and expanded polyglutamine (150Q) (12). These cell lines were named HD 16Q and HD 150Q, and their corresponding expressed proteins were named tNhtt-16Q and tNhtt-150Q. The cell lines were induced for 1 day with ponasterone A (1 μM) and then processed for immunoprecipitation by anti-GFP. In another experiment, we transfected the truncated ataxin-3 constructs to the neuro2a cell, and after 1 day, cells were collected and processed for immunoprecipitation by GFP antibody. Blots were sequentially probed with anti-ubiquitin and anti-GFP. As shown in Fig. 1*A*, truncated huntingtin with 150Q proteins or the truncated ataxin-3 with 80Q proteins were ubiquitinated, whereas those truncated proteins with normal glutamine repeats were not ubiquitinated. Fig. 1*B* showed the same blot as those in *A* after probing with GFP antibody. The tNhtt-150Q

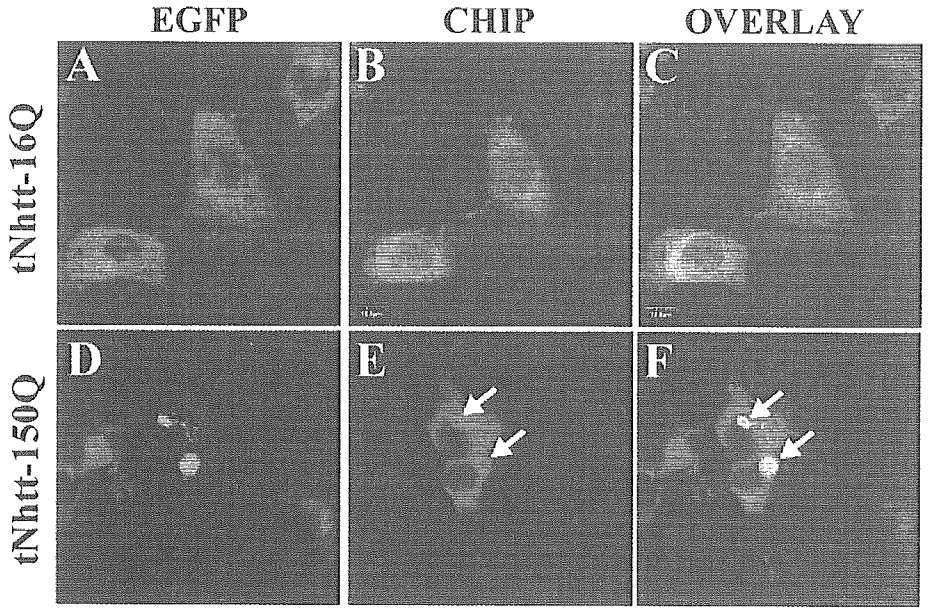

FIG. 3. **Recruitment of CHIP to the mutant huntingtin aggregates.** The HD 16Q (*A–C*) and HD 150Q (*D–F*) cells were transiently transfected with CHIP and induced in the similar way as described in the Fig. 2. Cells were then subjected to immunofluorescence staining with anti-v5. Cy3-conjugated secondary antibody was used to stain the CHIP. *Arrows* indicate the recruitment of CHIP to the huntingtin aggregates.

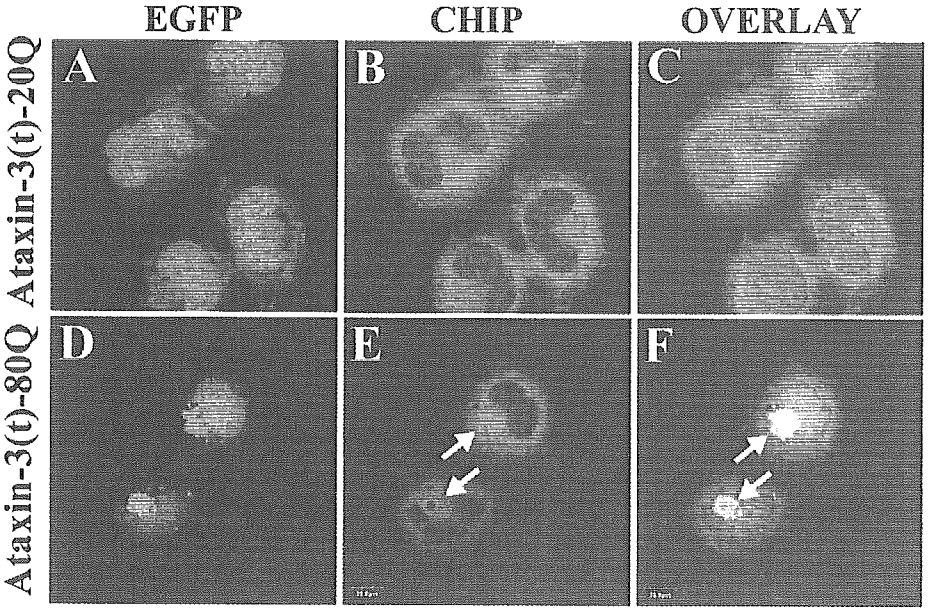

FIG. 4. **CHIP associates with the ataxin-3 aggregates.** The neuro2a cells were sequentially transfected with CHIP and truncated ataxin-3-EGFP fusion constructs containing 20Q (*A–C*) and 80Q (*D–F*). Forty-eight hours later, cells were processed for immunofluorescence staining using v5 antibody. Cy3-conjugated secondary antibody was used to stain the CHIP. *Arrows* indicate the recruitment of CHIP to the ataxin-3 aggregates.

appeared as multiple bands because of the instability of the CAG repeats.

CHIP Interacts with the Polyglutamine-expanded Truncated N-terminal Huntingtin or Ataxin-3—Because misfolding promotes the ubiquitination of the expanded polyglutamine proteins, we next wanted to know the identity of the ubiquitin ligase that is responsible for the misfolding-dependent ubiquitination. We first tested the possibility of CHIP ubiquitin ligase, because recently, CHIP has been shown to be responsible for the ubiquitination and degradation of the misfolded proteins. CHIP was transiently transfected into HD 16Q and HD 150Q cells, the cells were induced with ponasterone A for 1 day, and then the cell lysates were processed for immunoprecipitation by anti-GFP. In a similar experiment, CHIP was co-transfected along with a different truncated ataxin-3 construct, and then the cell lysates were processed for immunoprecipitation. In both experiments, blots were detected with anti-v5 antibody. As shown in Fig. 2, *A* and *C*, CHIP was immunoprecipitated with the truncated N-terminal huntingtin with 150Q and truncated ataxin-3 with 80Q but not the truncated N-terminal huntingtin with 16Q or truncated ataxin-3 with 20Q. Fig. 2, *B* and *D* showed the same blot as in Fig. 2, *A* and *C*, respectively, after detection with anti-GFP.

Association of CHIP with Polyglutamine Aggregates—Next

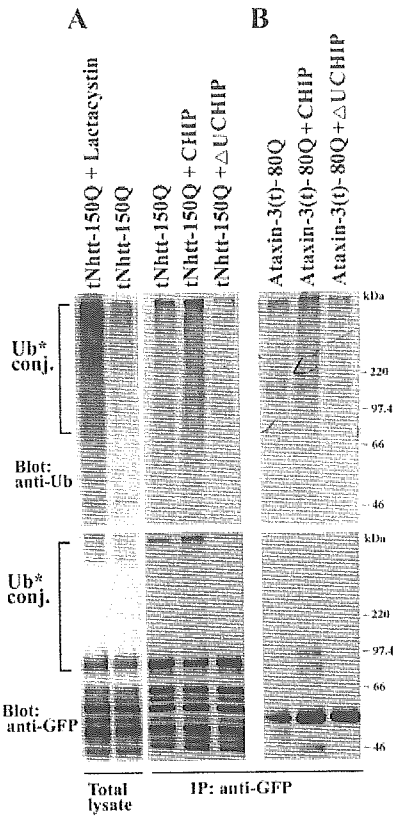

FIG. 5. **Involvement of CHIP in the ubiquitination of expanded polyglutamine proteins.** *A*, the HD 150Q cells were transiently transfected with full-length CHIP, U-box-deleted CHIP or the empty vectors (2 μg of each/well of 6-well tissue-cultured plate) and induced and processed for immunoprecipitation (*IP*) in the similar way as described in the Fig. 2. Blots were sequentially probed with anti-ubiquitin (*top blot*) and anti-GFP (*bottom blot*). In total lysate lanes, induced HD 150Q cells were left untreated or treated with 10 μM lactacystin for 8 h, and then the cell lysate were made and subjected to immunoblotting. *B*, neuro2a cells were first transfected with full-length CHIP, U-box-deleted CHIP, and empty vector (same amounts as used in *A*), and after 12 h, the cells were transfected again with truncated ataxin-3 constructs with 20Q and 80Q in the similar way as described in Fig. 2. The cell lysate were then processed for immunoprecipitation by anti-GFP followed by sequential immunoblotting with anti-ubiquitin (*top blot*) anti-GFP (*bottom blot*). *Ub* conj*, ubiquitin conjugates.

we checked the normal distribution and recruitment of CHIP to the polyglutamine aggregates. First we transiently transfected the CHIP into the HD 16Q and HD 150Q cells, and then the cells were induced to express the truncated huntingtin proteins. After 1 day of induction, cells were processed for immunofluorescence experiments using anti-v5 antibody. CHIP was normally localized into the cytosolic compartment in the wild type neuro2a cells or in the uninduced HD 16Q and HD 150Q cells (Fig. 3). Induction of the expression of the tNhtt-16Q protein did not alter the localization pattern of CHIP in the HD 16Q cell; however, the induction of tNhtt-150Q protein in the HD 150Q cell caused the recruitment of CHIP to the aggregates (Fig. 3). Next, we tested the similar redistribution of CHIP in the ataxin-3 aggregates. CHIP was co-transfected along with truncated ataxin-3 constructs and after 2 days of transfection, cells were processed for immunofluorescence experiments. As expected, CHIP was also recruited to truncated ataxin-3 aggregates (Fig. 4).

CHIP Enhances the Ubiquitination of Polyglutamine-expanded Truncated N-terminal Huntingtin or Ataxin-3—Because CHIP co-immunoprecipitates with expanded polyglutamine proteins and recruits the polyglutamine aggregates, we further tested its possible involvement in the ubiquitination of the expanded polyglutamine proteins. To test this hypothesis, we transfected CHIP (both full-length and U-box-deleted) to the HD 150Q cells, or co-transfected CHIP along with truncated ataxin-3 constructs. The cell lysate were then made and processed for immunoprecipitation by anti-GFP. Fig. 5 showed that CHIP enhanced the rate of ubiquitination of both truncated N-terminal huntingtin containing 150Q (Fig. 5*A*, *top blot*) as well as truncated ataxin-3 with 80Q (Fig. 5*B*, *top blot*). This enhanced rate of ubiquitination was prevented by the deletion of U-box of CHIP. The bottom blots of both Fig. 5, *A* and *B* are the same blots as the top blots, respectively, but probed with anti-GFP. Anti-GFP also detected smears of ubiquitinated derivatives of expanded polyglutamine proteins in the only CHIP-transfected cell lysate. The lactacystin-treated cell lysate was used as positive control to compare the CHIP-induced ubiquitination profile (Fig. 5*A*, *first two lanes*). Because the deletion of U-box of CHIP reduced the rate of ubiquitination, we further tested whether the U-box-deleted CHIP still associates with the polyglutamine aggregates. As shown in Fig. 6, U-box deleted CHIP also recruits to the huntingtin aggregates. We have also observed the association of U-box-deleted CHIP with the

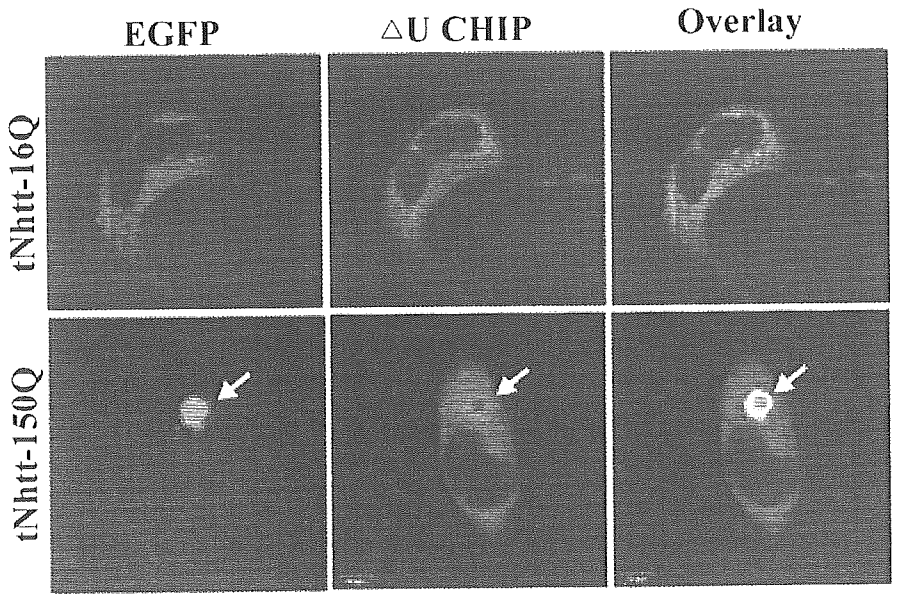

FIG. 6. **Association of U-box-deleted CHIP with the huntingtin aggregates.** The HD 16Q and HD 150Q cells were transiently transfected with U-box-deleted CHIP and induced in a similar way as described in the Fig. 2. Cells were then subjected to immunofluorescence staining with anti-v5. Cy3-conjugated secondary antibody was used to stain the CHIP. *Arrows* indicate the recruitment of U-box deleted CHIP to the huntingtin aggregates.

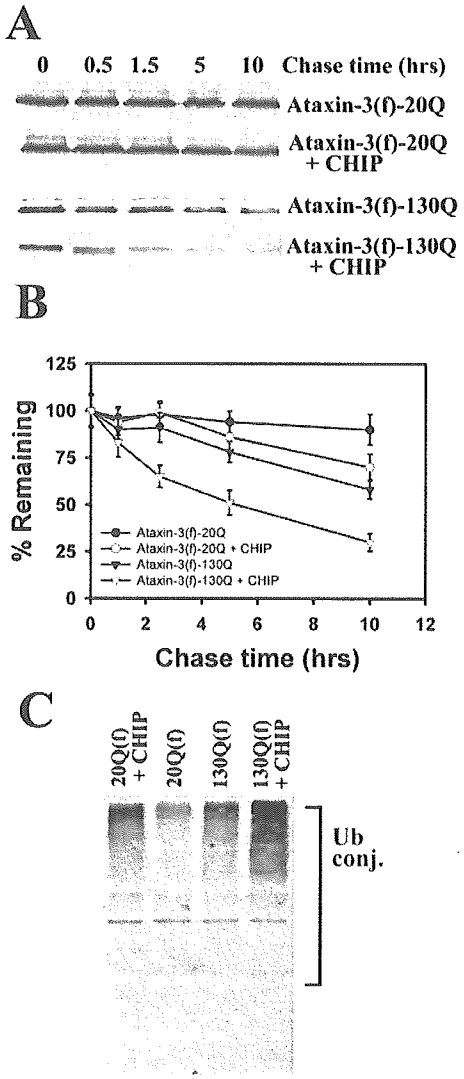

FIG. 7. **CHIP promotes degradation of polyglutamine-expanded proteins.** *A*, mouse neuro2a cells were transiently transfected with full-length ataxin-3 constructs (20Q and 130Q) either alone or along with CHIP. Twenty-four hours later, cells were chased in the presence of 10 μg/ml cycloheximide for different time periods as indicated in the figure. Cells were then collected and processed for immunoblotting using anti-GFP. *B*, quantitation of the band intensities of the blots collected from three independent experiments were performed using NIH Image analysis software. Values are means ± S.D. *C*, cells were transfected as described in *A*. Cells were collected and subjected to immunoprecipitation using anti-GFP. Blot was detected with anti-ubiquitin. *Ub* conj*, ubiquitin conjugates.

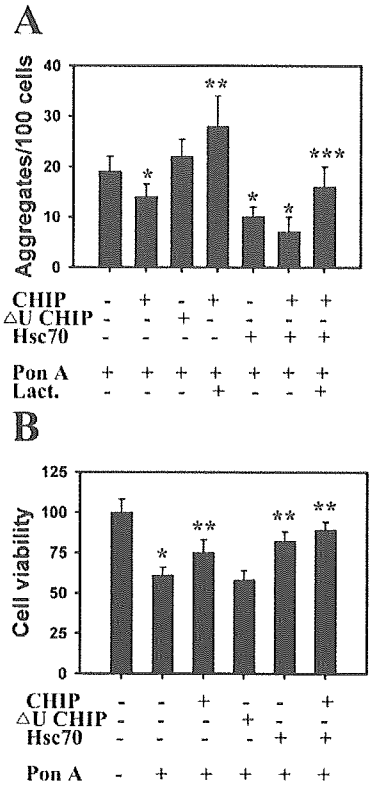

FIG. 8. **CHIP reduces the aggregate formation (*A*) and cell death (*B*) caused by expanded polyglutamine protein.** *A*, HD 150Q cells were transiently transfected with CHIP and U-box-deleted (*ΔU*) CHIP independently or together with Hsc70 (2 μg of each/well of 6-well tissue-cultured plate). Transfected DNA was equalized by using empty pcDNA vector. Twelve hours later, the medium was replaced, and then the cells were induced with 0.5 μM ponasterone A (*Pon A*). Aggregate counting was monitored 24 h after ponasterone A treatment in the fluorescence microscope as described under "Experimental Procedures." Lactacystin (*Lact.*) was used at a dose of 2.5 μM. Results are means ± S.D. of three independent experiments each performed triplicate. *, $p < 0.05$ as compared with control; **, $p < 0.01$ as compared with CHIP-transfected experiment; ***, $p < 0.01$ as compared with CHIP plus Hsc70-transfected experiment. *B*, HD 150Q cells were transiently transfected with CHIP and U-box deleted CHIP independently or together with Hsc70 as described under *A*. Cells were harvested and replated in the 96-well tissue cultured plate. The cells were then differentiated with 5 mM dbcAMP and induced with 1 μM ponasterone A for 3 days. Cell viability was measured by MTT assay. Values are means ± S.D. of two independent experiments each performed triplicate. *, $p < 0.01$ as compared with control; **, $p < 0.01$ as compared with ponasterone A treated experiments.

ataxin-3 aggregates (data not shown). Result strongly indicates that the CHIP associates with the expanded polyglutamine protein through its interaction with Hsc70.

CHIP Enhances the Degradation of Polyglutamine-expanded Proteins—Because CHIP enhanced the ubiquitination of polyglutamine-expanded proteins; we further checked their rate of degradation upon CHIP overexpression. For this experiment, we used full-length ataxin-3 with 20Q and 130Q, because full-length ataxin-3 with 130Q forms very few aggregates (~5–10% cells form aggregates) after 48 h of transfection. Neuro2a cells were transiently transfected with ataxin-3 constructs either alone or along with CHIP. Twenty-four hours later, cells were chased with cycloheximide. As shown in Fig. 7, *A* and *B*, full-length ataxin-3 with 20Q is not degraded; however, full-length ataxin-3 with 130Q is degraded after 1.5, 5, and 10 h of chase. Overexpression of CHIP enhanced the degradation of full-length ataxin-3 with 130Q. Overexpression of CHIP also slightly enhanced the degradation of ataxin-3 with 20Q (Fig. 7, *A* and *B*). Fig. 7*C* demonstrated that full-length ataxin-3 with 130Q was ubiquitinated, and CHIP overexpression enhanced the rate of ubiquitination.

CHIP Decreases the Aggregation and Cell Death Mediated by the Expanded Polyglutamine Proteins—Because CHIP promotes the ubiquitination of expanded polyglutamine proteins, we expected that its overexpression would increase the rate of degradation of expanded polyglutamine proteins by proteasomes. If so, CHIP should decrease the aggregation of polyglutamine proteins. Therefore, we next checked the effect of CHIP on the rate of aggregate formation and cell viability in the HD 150Q cells after different days of transfection. As shown in Fig. 8*A*, overexpression of CHIP reduced the polyglutamine-expanded tNhtt aggregation, and the suppressive effect is more prominent when the CHIP is overexpressed along with Hsc70.

The deletion of the U-box of the CHIP abolished the suppressive effect on aggregation. CHIP overexpression also decreased the aggregation of truncated ataxin-3 with 80Q (data not shown). This inhibitory effect of CHIP on aggregate formation was prevented by the proteasome inhibitor lactacystin. CHIP was also able to protect the polyglutamine protein-induced cell death, and again, the protective effect was more when the CHIP was overexpressed along with Hsc70 (Fig. 8*B*).

DISCUSSION

Ubiquitin is a well known marker of polyglutamine aggregates, but how and when polyglutamine aggregates are ubiquitinated is not yet known. The most likely hypothesis is that the expanded polyglutamine proteins are misfolded, and failure to refold might cause their ubiquitination before they are degraded by proteasome. Here we first demonstrated that the expanded polyglutamine proteins that are misfolded became ubiquitinated. Secondly, we identified CHIP ubiquitin ligase that is responsible for the misfolding-dependent ubiquitination of the expanded polyglutamine proteins. Finally, we showed that overexpression of CHIP reduces the aggregate formation and cell death mediated by expanded polyglutamine proteins.

Ubiquitination begins with the ATP-dependent activation of ubiquitin by an activating enzyme (E1). The ligation of ubiquitin to the substrate is then carried out by a specific complex composed of an ubiquitin-conjugating enzyme (E2) and ubiquitin protein ligase (E3) (14). The question now is how the misfolded polyglutamine protein is recognized by the ubiquitination machine and whether chaperones play any role. The expanded polyglutamine protein has been shown earlier to specifically interact with Hsc70/Hsp70 chaperones (9), and now we have shown that CHIP associates and ubiquitinates expanded polyglutamine proteins. Results suggest that the Hsc70/Hsp70 and CHIP both play a critical role in the process of ubiquitination of polyglutamine proteins. CHIP was first identified as an interacting protein with the C terminus of Hsp70 and shown to negatively regulated Hsp70 chaperone activity (15). Subsequently, CHIP was demonstrated to be a ubiquitin ligase of the U-box family (16, 17). Recent reports also demonstrated that CHIP is responsible for the misfolding-dependent ubiquitination and degradation of cystic fibrosis transmembrane regulator (18), glucocorticoid receptor (19), mutant copper/zinc superoxide dismutase 1 (20, 21), and Tau protein (22, 23) and therefore could be a general ubiquitin ligase for the misfolded proteins (24, 25).

We have also observed that the overexpression of CHIP inhibits polyglutamine protein aggregation and cell death and that the inhibitory effects are more prominent when CHIP is expressed along with the Hsc70 chaperone. The results suggests that polyglutamine proteins are degraded by proteasomes after they are ubiquitinated by CHIP and that the removal of polyglutamine proteins protects cells from their toxic effect. Others have reported similar findings (20–23) where they have shown that overexpression of CHIP reduced the aggregation and cell death mediated by mutant copper/zinc superoxide dismutase 1 or Tau protein. However, there are reports suggesting that the expanded polyglutamine proteins are not degraded efficiently by the proteasome and that also there is proteasomal malfunction in the expanded polyglutamine protein-expressing cells (11, 26). In both the cases, there could be an increased accumulation of ubiquitinated derivatives of expanded polyglutamine proteins. CHIP along with Hsc70 might enhance the rate of degradation by increasing the ubiquitination rate. Overexpression of CHIP along with Hsc70 could also conceivably have recovered proteasomal malfunction by reducing the burden of aggregated polyglutamine proteins as well as other misfolded proteins. Altogether, our results demonstrate that the CHIP along with Hsc70 promotes the ubiquitination and degradation of expanded polyglutamine proteins that ultimately leads to the suppression of aggregation and cell death.

REFERENCES

1. Zoghbi, H. Y., and Orr, H. T. (2000) *Ann. Rev. Neurosci.* **23,** 217–247
2. Sherman, M. Y., and Goldberg, A. L. (2001) *Neuron* **29,** 15–32
3. Lin, X., Cummings, C. J., and Zoghbi, H. Y. (1999) *Neuron* **24,** 499–502
4. Cummings, C. J., Mancini, M. A., Antalffy, B., DeFranco, D. B., Orr, H. T., and Zoghbi, H. Y. (1998) *Nat. Genet.* **19,** 148–154
5. Chai, Y., Koppenhafer, S. L., Shoesmith, S. J., Perez, M. K., and Paulson, H. L. (1999) *Hum. Mol. Genet.* **8,** 673–682
6. Chai, Y., Koppenhafer, S. L., Bonini, N. M., and Paulson, H. L. (1999) *J. Neurosci.* **19,** 10338–10347
7. Stenoien, D. L., Cummings, C. J., Adams, H. P., Mancini, M. G., Patel, K., DeMartino, G. N., Marcelli, M., Weigel, N. L., and Mancini, M. A. (1999) *Hum. Mol. Genet.* **8,** 731–741
8. Warrick, J. M., Chan, H. Y. E., Gray-Board, G. L., Chai, Y., Paulson, H. L., and Bonini, N. M. (1999) *Nat. Genet.* **23,** 425–428
9. Jana, N. R., Tanaka, M., Wang, G., and Nukina, N. (2000) *Hum. Mol. Genet.* **9,** 2009–2018
10. Cummings, C. J., Reinstein, E., Sun, Y., Antalffy, B., Jiang, Y-H., Ciechanover, A., Orr, H. T., Beaudet, A. L., and Zoghbi, H. (1999) *Neuron* **24,** 879–892
11. Jana, N. R., Zemskov, E. A., Wang, G., and Nukina, N. (2001) *Hum. Mol. Genet.* **10,** 1049–1059
12. Wang, G. H., Mitsui, K., Kotliarova, S. E., Yamashita, A., Nagao, Y., Tokuhiro, S., Iwatsubo, T., Kanazawa, I., and Nukina, N. (1999) *Neuroreport* **10,** 2435–2438
13. Wang, G. H., Sawai, N., Kotliarova, S. E., Kanazawa, I., and Nukina, N. (2000) *Hum. Mol. Genet.* **9,** 1795–1803
14. Ciechanover, A. (1998) *EMBO J.* **17,** 7151–7160
15. Ballinger, C. A., Connell, P., Wu, Y., Hu, Z., Thompson, L. J., Yin, L. Y., and Patterson, C. (1999) *Mol. Cell. Biol.* **19,** 4535–4545
16. Jiang, J., Ballinger, C. A., Wu, Y., Dai, Q., Cyr, D. M., Hohfeld, J., and Patterson, C. (2001) *J. Biol. Chem.* **276,** 42938–42944
17. Hatakeyama, S., Yada, M., Matsumoto, M., Ishida, N., and Nakayama, K. I. (2001) *J. Biol. Chem.* **276,** 33111–33120
18. Meacham, G. C., Patterson, C., Zhang, W., Younger, J. M., and Cyr, D. M. (2001) *Nat. Cell Biol.* **3,** 100–105
19. Connell, P., Ballinger, C. A., Jiang, J., Wu, Y., Thompson, L. J., Hohfeld, J., and Patterson, C. (2001) *Nat. Cell Biol.* **3,** 93–96
20. Choi, J. S., Cho, S., Park, S. G., Park, B. C., and Lee, D. H. (2004) *Biochem. Biophys. Res. Commun.* **321,** 574–583
21. Urushitani, M., Kurisu, J., Tateno, M., Hatakeyama, S., Nakayama, K., Kato, S., and Takahashi, R. (2004) *J. Neurochem.* **90,** 231–244
22. Petrucelli, L., Dickson, D., Kehoe, K., Taylor, J., Snyder, H., Grover, A., De Lucia, M., McGowan, E., Lewis, J., Prihar, G., Kim, J., Dillman, W. H., Browne, S. E., Hall, A., Voellmy, R., Tsuboi, Y., Dawson, T. M., Wolozin, B., and Hardy, J. H. (2004) *Hum. Mol. Genet.* **13,** 703–714
23. Hatakeyama, S., Katsumoto, M., Kamura, T., Murayama, M., Chui, D. H., Planel, E., Takahashi, R., Nakayama, K. I., and Takashima, A. (2004) *J. Neurochem.* **91,** 299–307
24. Demand, J., Alberti, S., Patterson, C., and Hohfeld, J. (2001) *Curr. Biol.* **11,** 1569–1577
25. Murata, S., Minami, Y., Minami, M., Chiba, T., and Tanaka, K. (2001) *EMBO Rep.* **2,** 1133–1138
26. Holmberg, C. I., Staniszewski, K. E., Mensah, K. N., Matouschek, A., Morimoto, R. I. (2004) *EMBO J.* **23,** 307–318

Cell, Vol. 121, 387–400, May 6, 2005, Copyright ©2005 by Elsevier Inc. DOI 10.1016/j.cell.2005.02.035

UV-Induced Ubiquitylation of XPC Protein Mediated by UV-DDB-Ubiquitin Ligase Complex

Kaoru Sugasawa,[1,2,9,*] Yuki Okuda,[1,3,9] Masafumi Saijo,[2,4] Ryotaro Nishi,[1,2,3,4] Noriyuki Matsuda,[5] Gilbert Chu,[6] Toshio Mori,[7] Shigenori Iwai,[8] Keiji Tanaka,[5] Kiyoji Tanaka,[2,4] and Fumio Hanaoka[1,2,4]

[1]Cellular Physiology Laboratory
RIKEN Discovery Research Institute
[2]Core Research for Evolutional Science and Technology
Japan Science and Technology Agency
Wako, Saitama 351-0198
[3]Graduate School of Pharmaceutical Sciences
[4]Graduate School of Frontier Biosciences
Osaka University
Suita, Osaka 565-0871
[5]Department of Molecular Oncology
Tokyo Metropolitan Institute of Medical Science
Bunkyo-ku, Tokyo 113-8613
Japan
[6]Department of Medicine and Biochemistry
Stanford University
Stanford, California 94305
[7]Radioisotope Center
Nara Medical University
Kashihara, Nara 634-8521
[8]Graduate School of Engineering Science
Osaka University
Toyonaka, Osaka 560-8531
Japan

Summary

The xeroderma pigmentosum group C (XPC) protein complex plays a key role in recognizing DNA damage throughout the genome for mammalian nucleotide excision repair (NER). Ultraviolet light (UV)-damaged DNA binding protein (UV-DDB) is another complex that appears to be involved in the recognition of NER-inducing damage, although the precise role it plays and its relationship to XPC remain to be elucidated. Here we show that XPC undergoes reversible ubiquitylation upon UV irradiation of cells and that this depends on the presence of functional UV-DDB activity. XPC and UV-DDB were demonstrated to interact physically, and both are polyubiquitylated by the recombinant UV-DDB-ubiquitin ligase complex. The polyubiquitylation altered the DNA binding properties of XPC and UV-DDB and appeared to be required for cell-free NER of UV-induced (6-4) photoproducts specifically when UV-DDB was bound to the lesion. Our results strongly suggest that ubiquitylation plays a critical role in the transfer of the UV-induced lesion from UV-DDB to XPC.

*Correspondence: sugasawa@riken.jp
[9]These authors contributed equally to this work.

Introduction

Nucleotide excision repair (NER) is a versatile DNA repair pathway that eliminates a wide variety of helix-distorting base lesions, including ultraviolet light (UV)-induced cyclobutane pyrimidine dimers (CPDs) and pyrimidine-pyrimidone (6-4) photoproducts (6-4PPs), as well as bulky adducts induced by numerous chemical compounds. Impaired NER activity is associated with several rare autosomal recessive disorders in humans, such as xeroderma pigmentosum (XP) and Cockayne syndrome (CS) (Friedberg, 2001; Hoeijmakers, 2001). XP patients are clinically characterized by cutaneous hypersensitivity to sunlight exposure and a predisposition to skin cancer. Seven NER-deficient genetic complementation groups of XP (XP-A to -G) and two groups of CS (CS-A and -B) have been identified, and all of the corresponding genes (*XPA*~*XPG*, *CSA*, and *CSB*) have now been cloned (for a review, see Bootsma et al. [1997]).

Mammalian NER consists of two distinct subpathways: global genome NER (GG-NER), which operates throughout the genome, and transcription-coupled NER (TC-NER), which specifically removes lesions on the transcribed DNA strand of active genes. A major difference between these two subpathways appears to be in the strategies they use to detect damaged bases. In TC-NER, RNA polymerase II stalls at damage sites and triggers the repair reaction (Tornaletti and Hanawalt, 1999). In contrast, in GG-NER, protein factors bind specifically to damage sites. Accumulating evidence indicates that the XP group C (XPC) protein plays an essential role in GG-NER-specific damage recognition (Riedl et al., 2003; Sugasawa et al., 1998; Volker et al., 2001).

The XPC protein exists in vivo as a heterotrimeric complex with one of the two mammalian homologs of *S. cerevisiae* Rad23p (HR23A or HR23B) and centrin 2 (Araki et al., 2001; Masutani et al., 1994; Shivji et al., 1994). This complex binds to various NER-type lesions in vitro, including UV-induced 6-4PP (Batty et al., 2000; Sugasawa et al., 2001). However, biochemical studies revealed that the XPC complex is a structure-specific DNA binding factor that appears to recognize a certain secondary structure of DNA rather than the lesions themselves (Sugasawa et al., 2002). These biochemical properties of XPC plausibly explain the detection by GG-NER of many structurally unrelated lesions.

UV-damaged DNA binding protein (UV-DDB) has been also implicated in the lesion recognition of GG-NER. UV-DDB is a heterodimeric complex consisting of DDB1 (p127) and DDB2 (p48). It has a much higher binding affinity and specificity for damaged DNA than XPC (Batty et al., 2000), particularly with regard to UV-induced 6-4PP (Fujiwara et al., 1999; Reardon et al., 1993; Treiber et al., 1992). Mutations in the *DDB2* gene cause the genetic complementation group E of XP, and the patients belonging to this group lack the damage binding activity of UV-DDB (Chu and Chang, 1988;

Hwang et al., 1998; Itoh et al., 2000; Nichols et al., 1996; Rapic'-Otrin et al., 2003).

Despite its capacity for detecting DNA damage with extremely high sensitivity, UV-DDB is not required for all types of GG-NER. For example, the cell-free NER reaction was successfully reconstituted without UV-DDB (Araújo et al., 2000; Mu et al., 1995), although it has stimulatory effects under certain conditions (Abou-sekhra et al., 1995; Wakasugi et al., 2001; Wakasugi et al., 2002). However, in XP-E cells lacking UV-DDB activity, while GG-NER of 6-4PP is only moderately impaired, the removal of CPD from the global genome is profoundly reduced (Hwang et al., 1999). Furthermore, ectopic expression of functional human DDB2 in rodent cells enhances GG-NER of CPD, thereby suppressing UV-induced mutagenesis (Tang et al., 2000). These findings strongly suggest that UV-DDB plays an important role in recognizing CPD for GG-NER. Upon local UV irradiation within the nucleus, UV-DDB translocates into the damaged area even in the absence of XPC (Wakasugi et al., 2002), suggesting that UV-DDB may function at an earlier step in GG-NER in order to assist XPC to find damaged sites. However, it remains to be elucidated how XPC and UV-DDB are functionally linked in terms of damage recognition for GG-NER. The precise role of the extremely high binding affinity UV-DDB has for 6-4PP also remains unclear.

Interestingly, UV-DDB has recently been found to be contained in a large complex with cullin 4A, Roc1, and COP9 signalosome, which are components of ubiquitin ligase (E3) (Groisman et al., 2003). Although UV-DDB-associated E3 appears to be activated upon UV irradiation of cells, the physiological substrates of E3 activity have not yet been determined. Here we present evidence that the UV-DDB-E3 complex ubiquitylates XPC in response to UV irradiation of cells. Our findings functionally link the two NER damage recognition factors and provide novel insights into the molecular mechanisms underlying damage recognition in GG-NER.

Results

UV-Induced Posttranslational Modification of XPC Protein

To examine the in vivo response of the XPC complex to UV irradiation, a series of immunoblot analyses was carried out. The SV40-transformed, normal human fibroblast cell line WI38 VA13 was UV or mock irradiated and then lysed with buffer containing 0.3 M NaCl and 1% Nonidet P40. When the resulting soluble and insoluble fractions were subjected to immunoblotting with anti-XPC antibodies (Figure 1A, lanes 1–4), slowly migrating heterogeneous bands (150–300 kDa) appeared in the soluble fraction from the UV-irradiated cells (lane 2). These bands with lower mobility were detected with two anti-XPC antibodies of different specificity but did not appear in similar fractions prepared from the XPC-deficient cell line XP4PASV (lanes 5–8). These findings indicate that the XPC protein undergoes posttranslational modification in response to UV irradiation of the cells.

To investigate the time course of this XPC band shift, WI38 VA13 cells were UV irradiated and then incubated for various time periods before cell fractionation. In this experiment, the cells were cultured in the presence of cycloheximide to inhibit de novo protein synthesis after UV irradiation. We confirmed that treatment of the cells with 0.1 mM cycloheximide inhibited the incorporation of [^{3}H]leucine almost completely within 1 hr (data not shown). As shown in Figure 1B, slowly migrating XPC species appeared as early as 5 min after irradiation, peaked around 60 min, and declined thereafter. In the same set of cell extracts, no detectable band shift was observed for HR23B, XPA, XPB, or DDB1 (Figure 1B) or for centrin 2 (data not shown).

The response of XPC in cells treated with various DNA-damaging agents other than UV was also examined (see Figure S1 in the Supplemental Data available with this article online). The shift in molecular weight of XPC upon treatment with X-rays or chemicals such as 4-nitroquinoline 1-oxide (4-NQO), which is often referred to as a UV mimetic agent, was either undetectable or much weaker than that induced by UV. The observed XPC modification thus appeared to be rather specific for UV irradiation.

The XPC Protein Is Ubiquitylated In Vivo

The observed mobility shift of XPC upon UV irradiation was large and heterogeneous, with apparent sizes differing by 20 to more than 100 kDa. This pattern raised the possibility that ubiquitylation might be involved in this band shift. To test this possibility, the UV-induced XPC modification was examined with mouse FM3A ts85 mutant cells, which have been shown to express a temperature-sensitive form of the ubiquitin-activating enzyme E1 (Finley et al., 1984; Matsumoto et al., 1983). When cultured at nonpermissive temperatures (>39°C), de novo ubiquitylation is greatly reduced in these cells. In agreement with this, the levels of monoubiquitylated histone H2A (uH2A) are severely reduced in ts85 cells cultured at 39.5°C (Figure 1D, lanes 10–12) but not in the mutant cells maintained at permissive temperatures (lanes 7–9) or in the wild-type, parental FM3A cells cultured at either temperature (lanes 1–6). The UV-induced band shift of XPC was not detected in ts85 cells cultured at 39.5°C (Figure 1D). Thus, the UV-induced modification of XPC depends on E1 activity.

To demonstrate the ubiquitylation of XPC more directly, we first established a stable transformant of the XPC-deficient cell line XP4PASV that expresses FLAG-tagged XPC at physiological levels. This FLAG-XPC protein showed a shift in molecular weight after UV irradiation that exactly matched the change in endogenous XPC in UV-irradiated WI38 VA13 cells (Figure S2A). In addition, GG-NER of 6-4PP was completely restored in this transformant (Figure S2B), confirming that the expressed FLAG-XPC functions normally in vivo. Hemagglutinin (HA)-tagged ubiquitin was transiently overexpressed in this transformant, and FLAG-XPC was immunoprecipitated. When the precipitated samples were subjected to immunoblotting with anti-HA antibody, ubiquitylated FLAG-XPC was detected, particularly when the transfected cells were UV irradiated before the extract preparation (Figure 1E, lane 8). A low level of ubiquitylation may have occurred in the unirradiated cells, presumably because of nonspecific ubiq-

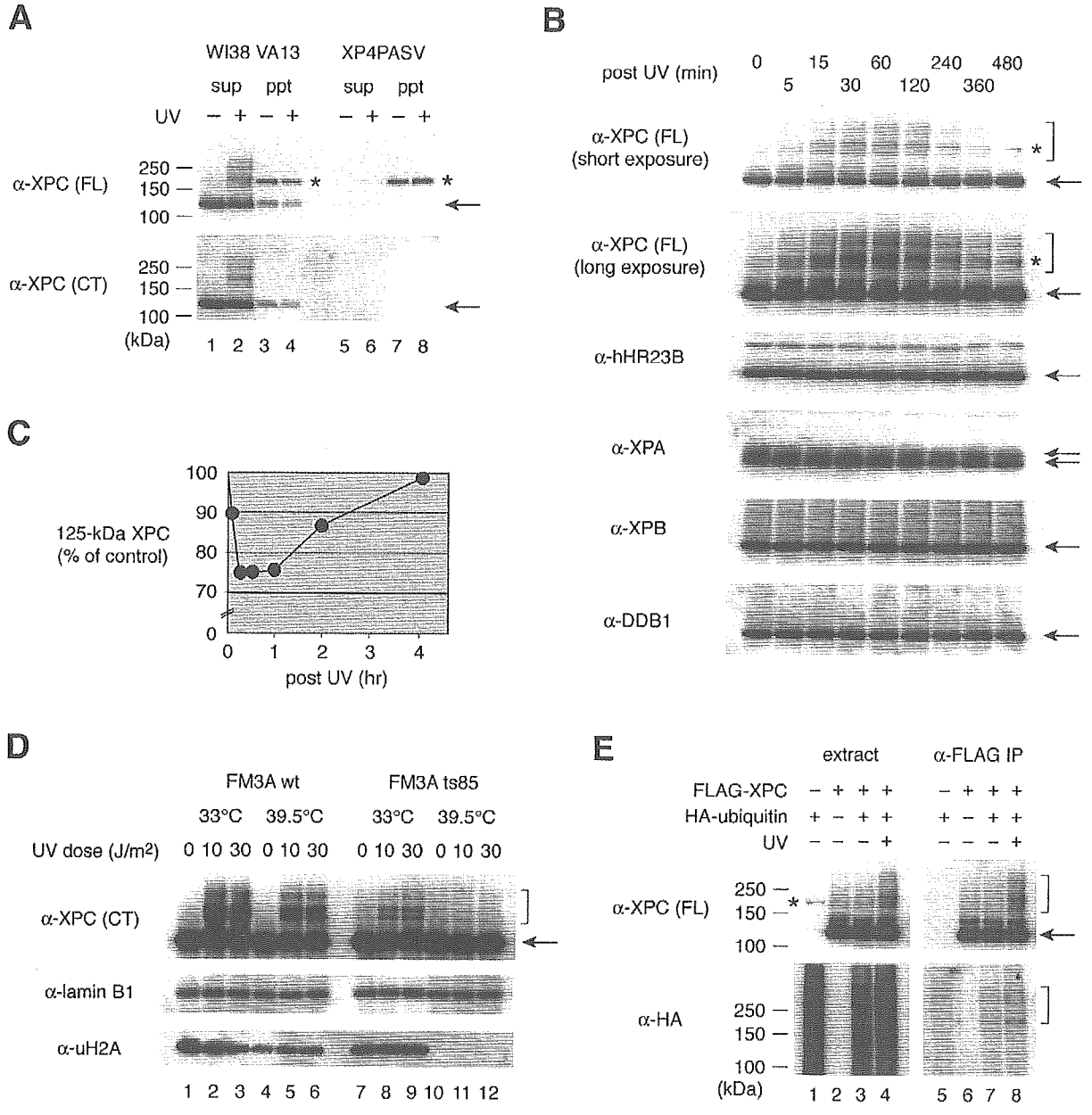

Figure 1. XPC Is Ubiquitylated in Response to UV Irradiation

(A) WI38 VA13 (normal) and XP4PASV (XPC-deficient) cells were UV irradiated at 10 J/m^2 or mock irradiated. After incubation at 37°C for 1 hr, soluble (sup) cell extracts, each containing 3 μg protein, as well as the corresponding amounts of the insoluble (ppt) fractions were subjected to immunoblot analyses using two different anti-XPC antibodies raised against the full-length (FL) protein or against a synthetic peptide corresponding to the C terminus (CT). The asterisk (also the asterisks in [B] and [E]) indicates nonspecific bands that crossreact with the anti-XPC (FL) antibody. The arrows (also the arrows in [D] and [E]) indicate the authentic unmodified XPC bands.

(B) WI38 VA13 cells were UV irradiated at 10 J/m^2 and incubated at 37°C in the presence of 0.1 mM cycloheximide for various times as indicated. The soluble cell lysates, each containing 3 μg protein, were subjected to immunoblot analyses with various antibodies as indicated. The arrows indicate the authentic bands for each NER protein. The brackets (also those in [D] and [E]) indicate the modified forms of XPC.

(C) The levels of 125 kDa XPC in each lane in (B) were quantified and normalized relative to the amount of hHR23B in the same lane. These values then were further normalized by the initial amount of the 125 kDa band and plotted as a graph.

(D) FM3A wild-type or ts85 cells were cultured for 16 hr at 33°C or 39.5°C, UV irradiated at the indicated doses, and cultured for another hour at the same temperature. Cell lysates were subjected to immunoblot analyses using the anti-XPC (CT) antibody. The same lysates were also immunoblotted for lamin B1 as a loading control and monoubiquitylated histone H2A (uH2A).

(E) The transformed XP4PASV cell line that stably expressed FLAG-XPC at physiological levels (XP4PASV/fXPC) was transiently transfected with an expression vector for HA-ubiquitin. Controls consisted of untransfected parental XP4PASV cells (lanes 1 and 5) and XP4PASV cells transfected with the vacant pCAGGS vector (lanes 2 and 6). At 7 hr of posttransfection, the cells were UV irradiated at 10 J/m^2 and incubated for another hour. Soluble cell extracts were prepared and subjected to immunoprecipitation with anti-FLAG M2 agarose. Aliquots of the cell extracts (3 μg protein; lanes 1–4) as well as the immunoprecipitates (lanes 5–8) were subjected to immunoblot analyses using the indicated antibodies.

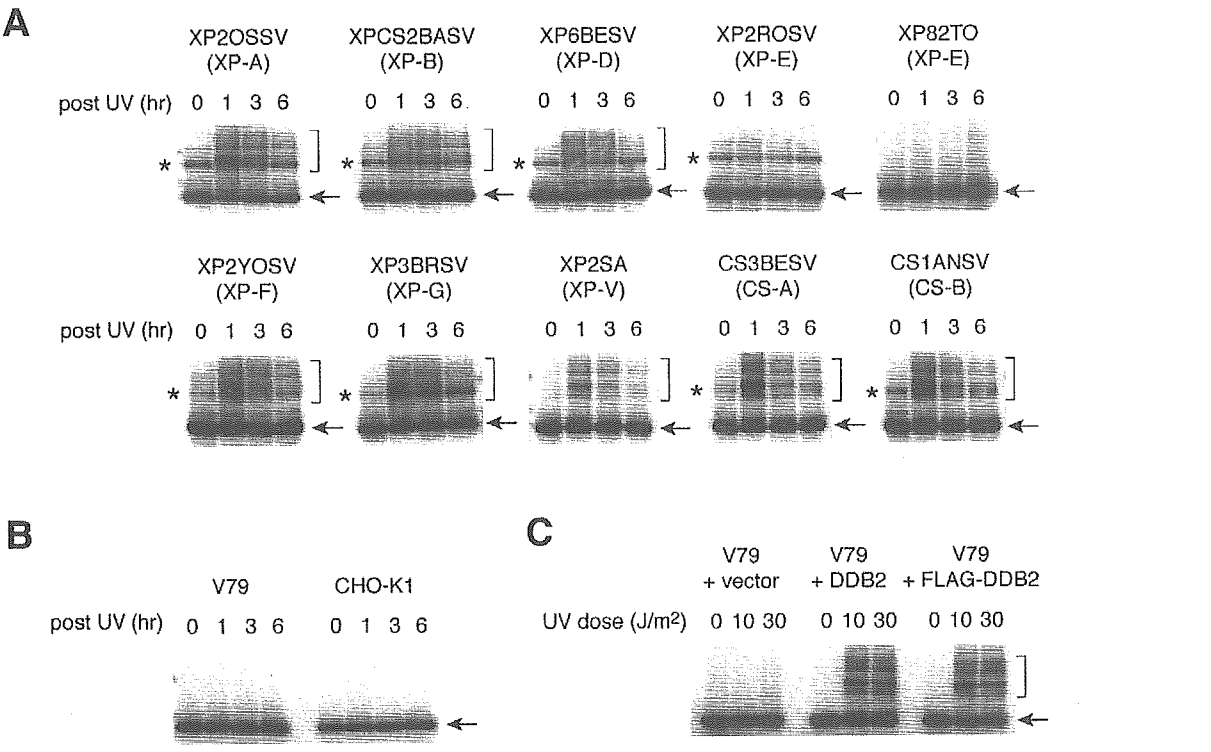

Figure 2. UV-Induced XPC Modification Depends on the Presence of Functional UV-DDB

(A) Cell lines derived from different XP and CS genetic complementation groups were UV irradiated at 10 J/m^2 and incubated at 37°C in the presence of 0.1 mM cycloheximide for various time periods. The soluble cell extracts (3 μg protein) were subjected to immunoblotting with anti-XPC (FL) antibody. The asterisks indicate nonspecific crossreacting bands that appear more evident in SV40-transformed cell lines than in the two untransformed cell lines XP82TO and XP2SA. The arrows and brackets (also those in [B] and [C]) indicate unmodified and modified forms of XPC, respectively.

(B) The Chinese hamster cell lines V79 and CHO-K1 were UV irradiated and cultured as described in (A). Cell lysates were prepared and subjected to immunoblot analysis using the anti-XPC (CT) antibody.

(C) Stable V79 transformants expressing human DDB2 (either untagged or FLAG-tagged), as well as a control transformant containing the vacant expression vector, were UV irradiated at the indicated doses and incubated at 37°C for 1 hr. Cell lysates were subjected to immunoblot analyses as described in (B).

uitylation caused by the overexpression of HA-ubiquitin (lane 7). From these data, we conclude that UV irradiation induces the ubiquitylation of XPC.

We found that, even when de novo protein synthesis was inhibited, the total amount of XPC was not significantly reduced after UV irradiation (Figure 1B). When we measured the levels of the authentic 125 kDa band of XPC, we found its levels dropped upon UV irradiation and then rose again later on when the shifted bands disappeared (Figure 1C). Therefore, the ubiquitylation of XPC appears to be reversible and does not serve as a signal for degradation.

UV-DDB Is Required for the Modification of XPC

To explore possible relationships between XPC modification and the NER process, we examined the UV-induced shift in molecular weight of XPC in human cell lines belonging to different genetic complementation groups of XP and CS. As shown in Figure 2A, most of the mutant cells exhibited normal band shifting of XPC upon UV irradiation. Intriguingly, however, the XPC band shift was not induced in two independent XP-E cell lines (Figure 2A). Both of these cells have mutations in the *DDB2* gene and lack UV-DDB activity (Nichols et al., 1996).

To further investigate the involvement of UV-DDB in XPC modification, Chinese hamster cell lines were used. Many established cell lines as well as primary lymphoid cells derived from Chinese hamsters lack UV-DDB activity (Hwang et al., 1998; Tang et al., 2000). As shown in Figure 2B, the two Chinese hamster cell lines we used, V79 and CHO-K1, were also defective in the UV-induced shift in molecular weight of XPC. UV-DDB activity is conferred to V79 cells when human *DDB2* gene is stably expressed (Tang et al., 2000). Interestingly, when human DDB2 (untagged or FLAG-tagged) was expressed in V79 cells, the XPC modification upon UV irradiation was restored (Figure 2C). We also confirmed that transient expression of wild-type human DDB2 but not its two point mutants (K244E and R273H) identified from XP-E patients complemented the defect of UV-induced XPC band shift in XP2ROSV cells (data not shown). These results indicate that UV-DDB activity is necessary for the UV-induced modification of XPC.

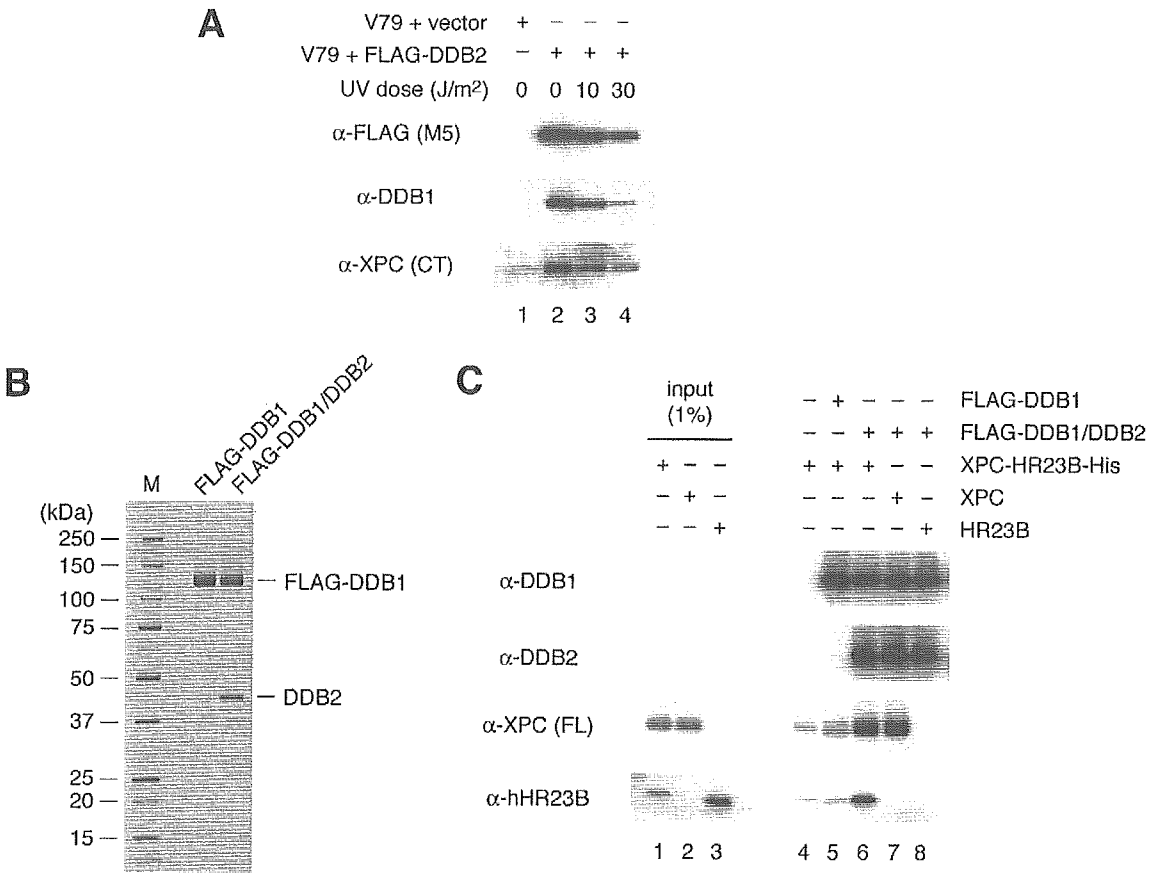

Figure 3. XPC Physically Interacts with UV-DDB

(A) The V79 transformant expressing FLAG-DDB2 was UV irradiated at the indicated dose (lanes 2–4). After incubation at 37°C for 1 hr, soluble cell extracts were prepared, FLAG-DDB2 was immunoprecipitated with anti-FLAG antibody beads, and aliquots of the bound fractions were subjected to immunoblot analyses with the indicated antibodies. As a negative control, the unirradiated, V79 transformant containing the vacant expression vector was processed in the same way (lane 1).

(B) Purification of recombinant UV-DDB. Purified FLAG-DDB1 (150 ng) and FLAG-DDB1/DDB2 heterodimer (200 ng) were subjected to SDS-PAGE (with a 4%–20% gradient gel) followed by silver staining. M, molecular weight markers.

(C) Anti-FLAG antibody beads (20 μl) prebound to either FLAG-DDB1 (1.3 μg) or FLAG-DDB1/DDB2 (1.8 μg) were incubated with XPC-HR23B-His (150 ng), XPC alone (103 ng), or HR23B alone (47 ng). After unbound materials were washed out, aliquots of the bound proteins were subjected to immunoblot analyses using the indicated antibodies (lanes 4–8). One percent of the input XPC and/or HR23B proteins were loaded onto the same gel as controls (lanes 1–3).

UV-DDB Physically Interacts with XPC

The above findings indicating some functional interaction between XPC and UV-DDB prompted us to examine whether they interacted physically as well. When FLAG-DDB2 in the stable V79 transformant was immunoprecipitated from soluble cell extracts, both DDB1 and endogenous XPC were coprecipitated (Figure 3A). This suggests that UV-DDB indeed interacts with XPC in vivo. This interaction was present in both unirradiated and irradiated cells, although UV irradiation significantly reduced the amount of UV-DDB and XPC that was precipitated. This is probably because UV-DDB becomes tightly bound to the UV-induced lesions and thus is not soluble during the extraction procedure (Otrin et al., 1997).

To demonstrate a direct interaction between XPC and UV-DDB, binding experiments were carried out using purified recombinant proteins. FLAG-DDB1 and DDB2 proteins were coexpressed in insect cells using the baculovirus system. With our baculovirus construct, FLAG-DDB1 was expressed in a large excess over DDB2, enabling us to separately purify the FLAG-DDB1/DDB2 complex and free FLAG-DDB1 from the same infected cell extract (Figure 3B). Either the purified UV-DDB complex or FLAG-DDB1 was bound to anti-FLAG antibody beads, which were then incubated with purified XPC-HR23B-His complex. A significant amount of XPC-HR23B-His coprecipitated with the UV-DDB complex, while its binding to FLAG-DDB1 alone was close to background levels (Figure 3C, compare lane 6 with lanes 4 and 5). This indicates that DDB2 is required for the interaction of UV-DDB with XPC. When XPC and HR23B were added separately to the UV-DDB heterodimer, only XPC was detected in the bound frac-

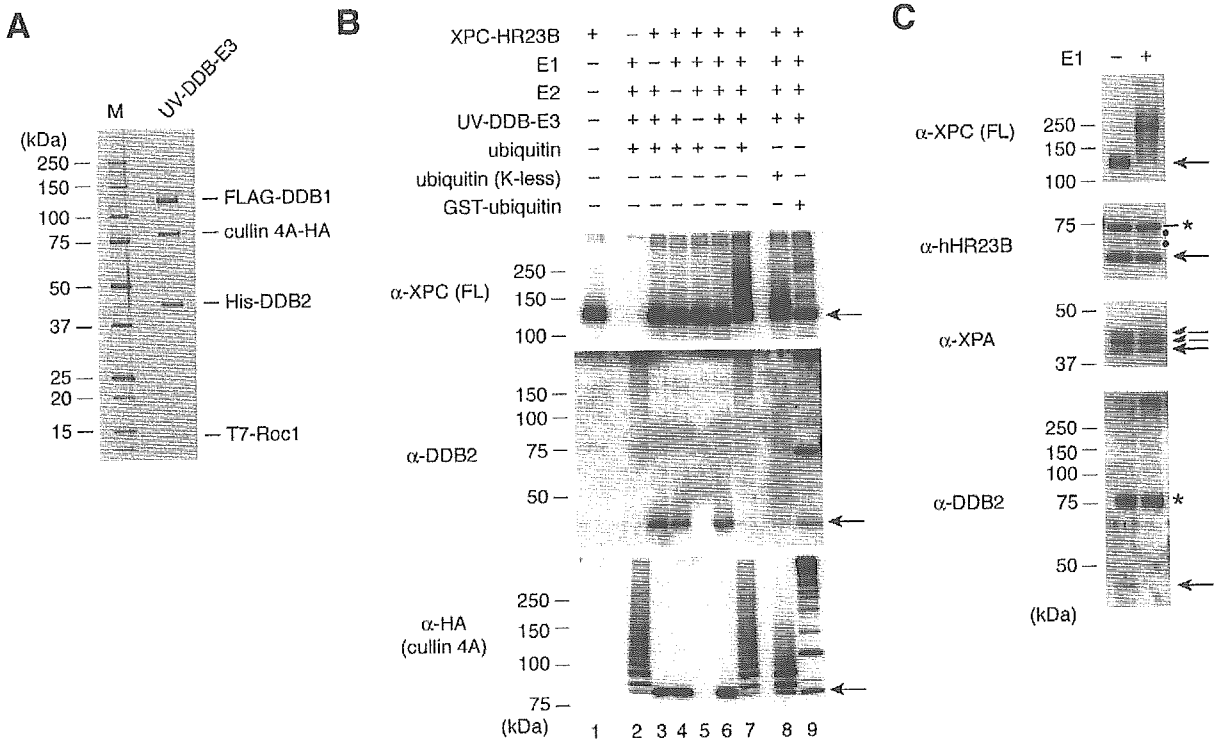

Figure 4. Cell-Free Ubiquitylation of XPC Mediated by the UV-DDB-E3 Complex

(A) The purified UV-DDB-E3 complex was subjected to SDS-PAGE (with a 4%–20% gradient gel) followed by silver staining. M, molecular weight markers.

(B) Cell-free ubiquitylation reactions were performed using the indicated sets of protein components. Where indicated, K-less ubiquitin (5 μg) or GST-ubiquitin (10 μg) was included instead of wild-type ubiquitin (lanes 8 and 9). Aliquots of the reaction mixtures were subjected to immunoblot analyses using the indicated antibodies. The arrows (also those in [C]) indicate the unmodified form of each protein.

(C) A mixture of XPC-HR23B-His (8 ng) and FLAG-XPA (5 ng) was included in the ubiquitylation reaction described in (B) in the absence or presence of E1. Aliquots of the reaction mixtures were subjected to immunoblotting with the indicated antibodies. The asterisk indicates nonspecifically crossreacting bands. The bands indicated by dots represent HR23B-His that had undergone low levels of ubiquitylation.

tion (lanes 7 and 8). These data demonstrate a direct physical interaction between XPC and UV-DDB.

The UV-DDB-E3 Complex Catalyzes the Ubiquitylation of XPC In Vitro

It has been recently reported that UV-DDB exists in vivo as a supercomplex containing cullin 4A and Roc1 that displays ubiquitin ligase (E3) activity (Groisman et al., 2003). This, together with our data, strongly suggests that the UV-DDB-E3 complex may be responsible for the ubiquitylation of XPC. To test this idea, cell-free ubiquitylation assays were carried out. The four subunits (DDB1, DDB2, cullin 4A, and Roc1) were expressed simultaneously in insect cells, and the heterotetrameric complex was purified (Figure 4A). When XPC-HR23B-His was incubated with this UV-DDB-E3 complex in the presence of E1, E2 (UbcH5a), ubiquitin, and ATP, a shift in the molecular weight of XPC was detected (Figure 4B). The shift appeared to depend on each of the protein components (lanes 2–7). The use of GST-tagged ubiquitin instead of normal ubiquitin resulted in an altered pattern of the shifted XPC bands (lane 9), strongly suggesting that the observed band shift is due to conjugation to ubiquitin. Furthermore, when a mutant ubiquitin in which all the lysine residues were changed to arginines (designated "K-less" ubiquitin) was employed in the reaction, the band shift was significantly reduced (lane 8), suggesting that the slow mobility species shown in lane 7 were the result of polyubiquitin chain formation. In the same reactions, DDB2 and cullin 4A were found to be ubiquitylated extensively as well, regardless of the presence or absence of XPC-HR23B-His (Figure 4B, lanes 2 and 7).

To examine the specificity of this in vitro ubiquitylation, XPC-HR23B-His and FLAG-XPA were simultaneously included in the reaction. While XPC and DDB2 were ubiquitylated extensively, little band shifting was observed with FLAG-XPA (Figure 4C) and DDB1 (data not shown) in the same reaction. Although a low percentage of HR23B-His appeared to be conjugated to one or two ubiquitin moieties (see bands indicated by dots in Figure 4C), the band shifting was nonetheless much less pronounced than XPC and DDB2. Thus, the in vitro ubiquitylation system appeared to retain similar substrate specificity as observed in the UV-irradiated cells (Figure 1B).

Since XPC and DDB2 were ubiquitylated in vitro by the same E3 complex, the in vivo fates of the two proteins after UV irradiation were compared. To do this,